Emergent many-body translational symmetries of Abelian and non-Abelian fractionally filled topological insulators

B. Andrei Bernevig[1] and N. Regnault[2]
[1]*Department of Physics, Princeton University, Princeton, New Jersey 08544, USA*
[2]*Laboratoire Pierre Aigrain, ENS and CNRS, 24 Rue Lhomond, FR-75005 Paris, France*
(Received 23 October 2011; published 27 February 2012)

The energy and entanglement spectrum of fractionally filled interacting topological insulators exhibit a peculiar manifold of low-energy states separated by a gap from a high-energy set of spurious states. In the current paper, we show that in the case of fractionally filled Chern insulators, the topological information of the many-body state developing in the system resides in this low-energy manifold. We identify an emergent many-body translational symmetry which allows us to separate the states in quasidegenerate center-of-mass momentum sectors. Within one center-of-mass sector, the states can be further classified as eigenstates of an emergent (in the thermodynamic limit) set of many-body relative translation operators. We analytically establish a mapping between the two-dimensional Brillouin zone for the fractional quantum Hall effect on the torus and the one for the fractional Chern insulator. We show that the counting of quasidegenerate levels below the gap for the fractional Chern insulator should arise from a folding of the states in the fractional quantum Hall system at an identical filling factor. We show how to count and separate the excitations of the Laughlin, Moore-Read, and Read-Rezayi series in the fractional quantum Hall effect into two-dimensional Brillouin zone momentum sectors and then how to map these into the momentum sectors of the fractional Chern insulator. We numerically check our results by showing the emergent symmetry at work for Laughlin, Moore-Read, and Read-Rezayi states on the checkerboard model of a Chern insulator, thereby also showing, as a proof of principle, that non-Abelian fractional Chern insulators exist.

DOI: 10.1103/PhysRevB.85.075128 PACS number(s): 74.20.Mn, 74.20.Rp, 74.25.Jb

I. INTRODUCTION

Band theory formed the foundation of solid-state physics for the past century. The theory analyzes the one-body motion of electrons through a crystal and obtains their wave functions as Bloch states dependent on a crystal momentum which takes values in a space equivalent to a d-dimensional torus (in d dimensions). Insulators hold a special place in band theory: At first look, they are its most boring aspect, having a full gap between occupied and unoccupied bands, no low-energy excitations, and hence no interesting properties at zero temperature. This viewpoint permeated the physics of much of the last century, but is, as we now know, untrue. The space of the eigenvectors of the Bloch Hamiltonians can be thought of as a unitary matrix, which in the case of insulators exhibits several gauge symmetries related to permutations of the occupied and unoccupied bands, thereby creating a complex manifold. The Hamiltonians can be regarded as maps from the Brillouin zone (BZ) to these manifolds, which, as mathematics teaches us, can be nontrivial. Anytime an insulator with a nontrivial map (Hamiltonian) is placed in the vicinity of the vacuum, gapless edge or surface states appear on the boundary and cross the energy space between the valence and conduction band. One of the first examples of such behavior was Haldane's Chern insulator model on the graphene lattice.[1] This model exhibits the physics of the integer quantum Hall (IQH) effect but does not have an overall applied magnetic field, thereby preserving the translational symmetry of the initial lattice. The IQH does not require any discrete symmetry to exist. The field of topological insulators has further evolved to include other symmetries such as time-reversal,[2–4] charge conjugation, and point-group symmetries.

Most of the research on topological insulators has focused on one-body electron Bloch physics. While several interesting works on insulators with interactions exist,[5–7] most of them focus on obtaining a mean-field state with topological properties through interactions. Recently, it has been proposed and substantiated[8–10] that fractionally filled bands of Chern insulators at $1/3$ and $1/5$ filing can exhibit an incompressible state in the same universality class as the Abelian $1/3$ and $1/5$ fractional quantum Hall (FQH) states. This state was dubbed the fractional Chern insulator (FCI). Its appearance is quite surprising, as the FQH and FCI problems vary considerably in several important ways, in the lack of a constant Berry curvature in the FCI, its large lattice filling, the absence of holomorphic and antiholomorphic (z,z^*) structures in the lowest band, and the presence of Umklapp processes that favor density wave states.

In a previous paper[8] we have shown that the ground state of the interacting $1/3$ fractionally filled band with Chern number 1 of the checkerboard Hamiltonian supports a threefold degenerate ground state separated by a gap from the excited states and which is a featureless liquid with momentum orbital occupation number $1/3$. We showed that the spectrum of quasiholes (spectrum at lower filling) by a gap separated into two manifolds: a high-energy uninteresting set of spurious states, and a low-energy set of quasiholes whose counting empirically matches that of the quasihole states in an Abelian $\nu = 1/3$ filling FQH state. Similar results were obtained for the particle entanglement spectrum,[11] a procedure used to obtain the topological part of the excitation spectrum directly from the ground-state wave function.[12] In the FCI, we have empirically found that the counting of states in the lower energy manifold, be they

ground states or quasiholes, exhibits a peculiar, yet undetermined structure. On a finite-size $N_x \times N_y$ lattice, a translationally invariant Hamiltonian for N_e electrons has a spectrum classified by total many-body lattice momenta $\sum_{i=1}^{N_e} k_{ix} (\mathrm{mod}\, 2\pi)$ and $\sum_{i=1}^{N_e} k_{iy} (\mathrm{mod}\, 2\pi)$, with each particle momentum $k_{ix,y}$ taking values $2\pi j/N_x, 2\pi l/N_y$, $j = 1, \ldots, N_x, l = 1, \ldots, N_y$. We have found that the counting of states in the low-energy (or entanglement energy) manifold per momentum sector exhibits multiple degeneracies, although the states themselves are not degenerate; there are no other exact degeneracies besides the point-group enforced ones, such as inversion. In many cases, we have found that an empirical Pauli principle borrowed from the FQH physics can sometimes (but not always) explain the degeneracies observed. While the degeneracy of some model wave functions has been worked out for the FQH effect on a lattice,[13] these results cannot be applied to the FCI.

Our prior analysis strongly suggests the existence of an emergent symmetry for FCIs at rational filling factors. In the present paper we show that such a symmetry is a many-body translational symmetry of the type exactly present in the FQH effect. We show analytically that, if the FCI state is in the same phase as the FQH state (including in the presence of quasiholes), the spectrum separates into quasidegenerate center-of-mass sectors which exhibit identical counting. Within each center-of-mass sector, the Hamiltonian eigenstates can be further classified as eigenstates of an emergent (in the thermodynamic limit) set of many-body relative translation operators. Using the recently obtained Girvin-MacDonald-Platzman (GMP)[14] algebra for Chern insulators[15] for the one-body density operators in the valence band, we build a set of many-body relative translational operators which diagonalize the Hamiltonian eigenstates in the lower manifold in the thermodynamic limit. We then establish an analytic mapping between the counting of zero-mode states in the FQH two-dimensional BZ on the torus (quasiholes) and that of the FCI levels in the low-energy manifold. We show that the counting of quasidegenerate levels below the gap for the FCI should arise from a folding of the zero-mode states in the FQH system at an identical filling factor. In the process, we show how to count and separate the quasihole excitations of the Read-Rezayi (RR)[16] series in the FQH effect into two-dimensional BZ momentum sectors and then how to map these into the momentum sectors of the FCI. We provide numerical verification for our analytic results by checking the emergent symmetry at work for Laughlin,[17] Moore-Read (MR),[18] and RR[16] states on the checkerboard model of a Chern insulator: We predict, from the FQH quasihole counting plus our FQH to FCI analytic mapping, the number of non-Abelian quasiholes per momentum sector in the FCI, and then check that it matches the numerical data obtained by exact diagonalization for large system sizes. Our work then also shows, as a proof of principle, that non-Abelian FCIs exist. The emergence of the low-manifold of states with folded FQH counting can be regarded as both a consequence as well as an imprint of the existence of the topological phase. Its existence is rather mysterious, as the GMP one-body algebra from which the many-body generators are built is not valid at large momentum[15] and is not in one-to-one mapping with the algebra of the continuum FQH problem.

The paper is organized as follows. In Sec. II we analyze the interacting Landau level problem on the torus in the continuum and obtain the set of many-body relative and center-of-mass symmetries that can classify the interacting spectrum by two-dimensional BZ of $N \times N$ momenta, where $N = GCD(N_\phi, N_e)$. GCD stands for greatest common denominator, N_ϕ is the number of fluxes that pierce the FQH torus due to the presence of the magnetic field, while N_e is the number of electrons. This section has no new material, most of the end results having been obtained by Haldane in a classic PRL,[19] but it does derive the physical equations in a much greater level of detail. We then reformulate the translational symmetry in terms of density operators, allowing a closer analogy with the FCI. We also explicitly show how to implement the many-body symmetries to build the FQH Hilbert space. Section III describes the counting of the zero modes of several pseudopotential Hamiltonians per two-dimensional BZ momentum. We focus on the RR series and show how the generalized Pauli principle that allows the counting of the quasihole states in the one-dimensional orbital space on the torus can be tuned to give the counting of zero modes in the two-dimensional BZ. As such, resolving the zero-modes (quasiholes) of model Haldane pseudopotential Hamiltonians in the two-dimensional BZ becomes a combinatorics problem of counting partitions. In Sec. IV we first rederive the commutator algebra of the projected densities in the lowest band of the Chern insulator on a $N_x \times N_y$ lattice first derived in Ref. 15, which reduces, in the long-wavelength, limit to the GMP algebra for the FQH effect for $N_\phi = N_x \cdot N_y$. We show that the noncommutativity of the projected densities which gives rise to the GMP algebra is a requirement in the Chern insulator, while in the trivial insulator the projected densities are adiabatically continuable to commuting variables in the atomic limit. We then show that the existence of a GMP algebra superimposed on a lattice of $N_x \times N_y$ sites implies the existence of many-body relative translational operators which classify many-body states by a two-dimensional momentum in a reduced BZ of $GCD(N_x, N_e) \times GCD(N_y, N_e)$ momenta. If the FCI phase is identical to that of the FQH, there is an emergent, center-of-mass degeneracy of $N_x/GCD(N_x, N_e)$ in the x direction and $N_y/GCD(N_y, N_e)$ in the y direction. We show that the counting of states in lower-energy manifold of the FCI is a folding of the counting of zero modes in the $N \times N$ BZ of the FQH times the difference between the center-of-mass degeneracies. We establish the analytic mapping between the FQH and FCI counting, and give several examples of this counting for several Abelian and non-Abelian RR states based on the generalize Pauli principle. We refer the reader versed in FQH translational symmetries to read this section and look at Figs. 2–4 for a simple understanding of how the FQH-FCI map works. In Sec. V we engage in extensive numerical calculations of both energy and entanglement spectra that show the existence of Laughlin, MR, and $\mathbb{Z}_3$ RR states on the checkerboard model[20] of the Chern insulator. We then show that the counting of quasihole states per momentum sector obtained in numerics matched the one derived by our analytic map for all our large set of data and parameters (lattice aspect ratios, electron numbers) tried. Up to the largest sizes available

on today's computers, the numerical data supports our analytic result.

II. MANY-BODY SYMMETRIES OF THE INTERACTING ELECTRONS IN A MAGNETIC FIELD

In this section, we aim to analyze the symmetries of the interacting Hamiltonian of electrons on a two-dimensional torus in the presence of a magnetic field and electron-electron interaction,

$$H = \frac{1}{2m}\sum_{j}^{N_e}\Pi_j^2 + \frac{1}{2}\sum_{i\neq j}^{N_e} V(\vec{r}_i - \vec{r}_j), \tag{1}$$

with $\Pi_j = -i\hbar\nabla_j - eA(r_j) = -i\hbar\nabla_j + |e|A(r_j)$ the canonical momentum in the presence of a magnetic field. N_e is the number of electrons in the system. We choose not to gauge fix and have $\vec{\nabla}\times\vec{A} = \vec{B}$. The positions of the particles, $\{\vec{r}_i\}$, reside on a two-dimensional torus of generators $\vec{L}_1$, $\vec{L}_2$. The Hamiltonian is periodic under translations by these vectors, $V(\vec{r}_i - \vec{r}_j) = (\vec{r}_i - \vec{r}_j + \vec{L}_{1,2})$, and can be written as a sum over the allowed reciprocal vectors $\vec{q}$:

$$\sum_{i\neq j}^{N_e} V(\vec{r}_i - \vec{r}_j) = \frac{1}{2\mathcal{A}}\sum_{\vec{q}} V(\vec{q})\sum_{i<j} e^{i\vec{q}\cdot(\vec{r}_i - \vec{r}_j)}, \tag{2}$$

where $\mathcal{A} = |\vec{L}_1\times\vec{L}_2|$ is the area of the unit cell, and $\vec{q} = m\vec{q}_1 + n\vec{q}_2$, $m,n\in\mathbb{Z}$ and $\vec{q}_1 = \frac{2\pi}{\mathcal{A}}\vec{L}_2\times\hat{z}$, $\vec{q}_2 = -\frac{2\pi}{\mathcal{A}}\hat{z}\times\vec{L}_1$. We now analyze the single- and many-body translational symmetries of the above Hamiltonian.

A. Guiding center coordinates and translational symmetries of the one-body problem

We first consider a $N_e = 1$ problem and try to find the symmetries of the one-body problem. A perfectly good translational operator could be $e^{i\vec{a}\cdot\vec{\Pi}}$, which would translate the single-body wave function by $\vec{a}$. However, this operator does not commute with the Hamiltonian because

$$[\Pi_\alpha,\Pi_\beta] = -i\hbar F_{\alpha\beta} \tag{3}$$

[where $F_{\alpha\beta} = \partial_\alpha A_\beta - \partial_\beta A_\alpha$ is the (magnetic) field strength applied on the sample]. Hence, the Hamiltonian wave functions cannot acquire quantum numbers under this operator and one finds an operator which commutes with Hamiltonian

$$K_\alpha = \Pi_\alpha - \frac{\hbar}{l^2}(\hat{z}\times\vec{r})_\alpha, \tag{4}$$

where $l = \sqrt{\hbar/eB}$ is the magnetic length. The commutation relations read

$$[K_\alpha,K_\beta] = 2i\frac{\hbar^2}{l^2}\epsilon_{\beta z\alpha} - i\hbar e(\partial_\alpha A_\beta - \partial_\beta A_\alpha) = i\frac{\hbar^2}{l^2}\epsilon_{z\alpha\beta}, \tag{5}$$

where we have used $B_\theta = \frac{1}{2}\epsilon_{\theta\alpha\beta}F_{\alpha\beta}$ as the uniform magnetic field applied on the sample. By direct calculation, we have for the commutators:

$$[K_\alpha,\Pi_\beta] = 0 \rightarrow [K_\alpha,H] = 0. \tag{6}$$

$\vec{K}$ is called guiding center momentum. Hence, the operator that implements the magnetic translation is

$$T(\vec{a}) = \exp\left(\frac{i}{\hbar}\vec{a}\cdot\vec{K}\right). \tag{7}$$

If translations by different vectors would mutually commute, we could form momentum eigenstates of the system. However, they do not. Using the operator relation $e^{A+B} = e^Ae^Be^{-\frac{1}{2}[A,B]}$, valid when $[A,[A,B]] = [B,[A,B]] = 0$ (which is the case here as the commutator of two guiding center momenta is a constant for uniform $\vec{B}$), we find

$$T(\vec{a}+\vec{b}) = T(\vec{b})T(\vec{a})e^{-\frac{1}{2\hbar^2}a_\alpha b_\beta[K_\alpha,K_\beta]} = T(\vec{b})T(\vec{a})e^{-\frac{i}{2l^2}\hat{z}\cdot(\vec{a}\times\vec{b})}, \tag{8}$$

which leads to

$$[T(\vec{a}),T(\vec{b})] = -2\sin\left(\frac{1}{2l^2}\hat{z}\cdot(\vec{a}\times\vec{b})\right)T(\vec{a}+\vec{b}). \tag{9}$$

This is called the magnetic translation algebra or GMP algebra. This algebra leads to the quantization of flux passing through the lattice: Going around the unit cell must give us the identity (same condition as commutators of $\vec{L}_1$, $\vec{L}_2$ translations must commute). This GMP algebra arises in several contexts in the quantum Hall effect and has the interpretation of a quantum deformation of the classical algebra of area-preserving diffeomorphisms on the plane as well as that of magnetic translations in a uniform field as discussed. Integer quantum Hall states are invariant under area-preserving diffeomorphisms. In finite size, the GMP algebra is the Lie algebra of $U(N_\Phi)$. Combinations (powers and products) of the operators of the algebra commute with the interacting Hamiltonian and can hence be simultaneously diagonalized giving the good quantum numbers of the problem. Our scope is to find the maximal set of such good quantum numbers for a translationally invariant interacting electrons in the presence of a magnetic field.

We now particularize (without loss of generality, since one can always deform the BZ to a rectangle) to $\vec{L}_1 = L_x\hat{x}, \vec{L}_2 = L_y\hat{y}$:

$$T(L_x\hat{x})T(L_y\hat{y})T(-L_x\hat{x})T(-L_y\hat{y}) = 1 = e^{\frac{i}{l^2}L_xL_y}. \tag{10}$$

Hence, $L_xL_y = 2\pi l^2N_\phi$ or, for a nonrectangular lattice, $\frac{1}{l^2}\hat{z}\cdot(\vec{L}_1\times\vec{L}_2) = 2\pi N_\phi$. For this quantization condition, we have that $[T(\vec{L}_1),T(\vec{L}_2)] = 0$. N_ϕ is the number of magnetic flux quanta passing through a unit cell. As a spoiler for the Chern insulator section, notice that this is the same as the number of sites N_s on a square lattice with lattice constant $a_0 = \sqrt{2\pi l^2}$ and number of sites in the x direction L_x/a_0 and in the y direction L_y/a_0. Hence, the magnetic field to Chern insulator lattice analogy is $L_x/\sqrt{2\pi l^2}\rightarrow N_x$, $L_y/\sqrt{2\pi l^2}\rightarrow N_y$, $N_\phi\rightarrow N_s$. Observe that $L_x/\sqrt{2\pi l^2}\rightarrow N_x$, $L_y/\sqrt{2\pi l^2}\rightarrow N_y$, $N_\phi\rightarrow N_s$ are all integers.

B. Many-body translational symmetries

We now focus on the interacting problem. The many-body problem is characterized by translation operators for each ith

particle, $T_i(\vec{a})$. Translational operators of different particles commute:

$$[T_i(\vec{a}),T_j(\vec{b})] = -2\delta_{ij}T_i(\vec{a}+\vec{b})\sin\left(\frac{1}{2l^2}\hat{z}\cdot(\vec{a}\times\vec{b})\right). \quad (11)$$

Physical quantities are invariant under magnetic translations *of any particle i* by a linear combination of multiples of L_x,L_y:

$$\vec{L}_{mn} = \{m\vec{L}_1 + n\vec{L}_2,\ m,n \in \mathbb{Z}\}. \quad (12)$$

Following Haldane,[19] primitive translations $\vec{L}_{mn}$ are those for which $\lambda\vec{L}_{mn}$, $0<\lambda<1$ are not lattice vectors; hence, (m,n) have no common divisors. Choose a potential $V(r+L_a) = V(r)$ such that the whole Hamiltonian commutes with the translation operators $T_i(\vec{L}_1),T_i(\vec{L}_2)$ for each particle $i = 1,\ldots,N_e$. This means that the wave functions of the Hamiltonian are eigenstates of the translation operator up to a phase:

$$T_i(\vec{L}_j)\psi_\alpha(\vec{r}_i) = \psi_\alpha(\vec{r}_i+\vec{L}_j) = e^{i\theta^i_j}\psi_\alpha(\vec{r}_i), \quad (13)$$

where i is the particle index, $j=1,2$, and θ^i_j are the eigenvalues. In the wave function $\psi_\alpha(\vec{r}_i)$, we have suppressed the position of all other particles but the ith, as they do not get translated by T_i. Let $T_i(\vec{L}_{mn})$ be the translation operator that translates the ith particle by the primitive translation $\vec{L}_{mn} = m\vec{L}_1 + n\vec{L}_2$:

$$T_i(\vec{L}_{mn})\,|\psi_\alpha\rangle = e^{i\theta^i_{mn}}\,|\psi_\alpha\rangle\,. \quad (14)$$

The eigenvalue θ^i_{mn}, which we will encounter again, can be expressed in terms of the eigenvalues of the primitive translations by $\vec{L}_1,\vec{L}_2$, θ^i_1,θ^i_2:

$$\begin{aligned} T_i(\vec{L}_{mn}) &= T_i(m\vec{L}_1+n\vec{L}_2) = T_i(m\vec{L}_1)T_i(n\vec{L}_2)e^{i\hat{z}\cdot(\vec{L}_1\times\vec{L}_2)\frac{mn}{2l^2}} \\ &= (T_i(\vec{L}_1))^m(T_i(\vec{L}_2))^n e^{i\pi N_\phi mn}. \end{aligned} \quad (15)$$

Hence, the eigenvalue of translation by $\vec{L}_{mn}$ is $\theta^i_{mn} = \pi mnN_\phi + m\theta^i_1 + n\theta^i_2$. Since eigenstates are symmetric or antisymmetric under exchange of identical particles i,j, we have that $e^{i\theta^i_{mn}} = e^{i\theta^j_{mn}} = e^{i\theta_{mn}}$: The eigenvalues of the translation operators for particle i do not depend on the particle chosen. The Hilbert space of the problem is separated in different sectors labeled by θ_1,θ_2. At this point, the analysis of the symmetries of the problem under translational invariance by each particle has run its course. Haldane[19] showed how to now introduce the many-body formalism for the translation operators. We expand his description in detail below.

Consider N_e electrons on a torus pierced by N_ϕ fluxes, such that the filling factor $\nu = N_e/N_\phi$ is a rational number p/q, with $(p,q)=1$ relatively prime. Let $N_e = pN$, $N_\phi = qN$, where $GCD(N_e,N_\phi) = N$. One thing we can hope from a many-body formulation of the translation operators is to separate the many-body problem into its center-of-mass part and a relative coordinate part. The center-of-mass operator moves each and every particle by the same amount:

$$T_{\rm CM}(\vec{a}) = \prod_{i=1}^{N_e} T_i(\vec{a}). \quad (16)$$

The center-of-mass translation by an arbitrary quantity commutes with the Hamiltonian but does not commute with the single-particle translation operators $T_i(\vec{L}_j)$ and hence does not keep us in a Hilbert space specified by θ_1,θ_2. To find the center-of-mass operators act within the same Hilbert space, we look for all $\vec{a}$ for which the center-of-mass operator $T_{\rm CM}(\vec{a})$ commutes with every $T_i(\vec{L}_j)$. Since operators of different particles commute, this is tantamount to imposing the constraint

$$[T_i(\vec{a}),T_i(\vec{L}_j)] = -2T_i(\vec{a}+\vec{L}_j)\sin\left(\frac{1}{2l^2}\hat{z}\cdot(\vec{a}\times\vec{L}_j)\right) = 0. \quad (17)$$

Hence, the condition for vanishing commutator is $\hat{z}\cdot(\vec{a}\times\vec{L}_j) = 2l^2\pi r$. Since $\vec{L}_1,\vec{L}_2$ span the two-dimensional plane, it is clear that any vector in the plane can take the form $\vec{a} = \alpha\vec{L}_1 + \beta\vec{L}_2$, where α,β are real numbers. Taking $j=2$ in Eq. (17) we have $\alpha\hat{z}\cdot(\vec{L}_1\times\vec{L}_2) = 2\pi l^2 r = \alpha 2\pi l^2 N_\phi$. Hence, $\alpha = r/N_\phi$, and similarly, by taking $j=1$, for β. Hence, the most general center-of-mass motion which leaves the system invariant is $T_{\rm CM}(\vec{L}_{mn}/N_\phi)$. All other forms of center-of-mass translation change the Hilbert space of the system.

Our purpose now is to separate the motion of the system into a center-of-mass motion and a relative motion of the particles. Toward this, Haldane[19] defined the relative translation operator $\tilde{T}_i$ acting on particle i so that the motion of that particle is compensated by the motion of all other particles in the opposite direction:

$$\begin{aligned} \tilde{T}_i(\vec{a}) = \prod_{j=1}^{N_e} T_i(\vec{a}/N_e)T_j(-\vec{a}/N_e) = T_i((N_e-1)\vec{a}/N_e) \\ \times \prod_{j=1,j\neq i}^{N_e} T_j(-\vec{a}/N_e). \end{aligned} \quad (18)$$

Since $T_i(\vec{a})T_i(-\vec{a}) = 1$, the relative translation operator of the system has the property that $\prod_{i=1}^{N_e}\tilde{T}_i(\vec{a}) = 1$. When $\tilde{T}_i(\vec{a})$ applied to a function of $\vec{r}_i - \vec{r}_j$ $(i\neq j)$, it translates the function by $\vec{a}$; when applied to a function of $\vec{r}_j - \vec{r}_k$ $(k,j,\neq i)$, it does nothing. Due to the periodicity of the interaction term, only $\tilde{T}_i(\vec{L}_{mn})$ commute with the Hamiltonian. We have introduced the center-of-mass operator and the relative translation operator, so it seems natural that the total translation operator factorizes in a product of the two:

$$\begin{aligned} T_i(\vec{a}) &= T_{\rm CM}\left(\frac{\vec{a}}{N_e}\right)\tilde{T}_i(\vec{a}) \\ &= \prod_{j=1,j\neq i}^{N_e} T_j\left(\frac{\vec{a}}{N_e}\right)T_j\left(-\frac{\vec{a}}{N_e}\right)T_i\left(\frac{\vec{a}}{N_e}\right)\left[T_i\left(\frac{\vec{a}}{N_e}\right)\right]^{N_e-1}. \end{aligned} \quad (19)$$

The relative translation operator commutes with any center-of-mass translation for any $\vec{a},\vec{b}$:$[\tilde{T}_i(\vec{a}),T_{\rm CM}(\vec{b})] = 0$, a clear indication that both of them are diagonalizable at the same time. To review the bidding, we have introduced center-of-mass translations $T_{\rm CM}(\vec{a})$ which commute with the Hamiltonian, found the ones $[T_{\rm CM}(\vec{L}_{mn}/N_\phi)]$ which commute with the single-particle translation operators $T_i(\vec{L}_j)$, even though, as we will see, the $T_{\rm CM}(\vec{L}_{mn}/N_\phi)$ do not necessarily

commute between themselves, and found the relative momentum operators which commute with the Hamiltonian and with the center-of-mass translations.

We would like to simultaneously diagonalize the relative translation operators and the Hamiltonian, and are hence after the maximal set of $\tilde{T}_i(\vec{a})$ which commute with each other $[\tilde{T}_i(\vec{a}),\tilde{T}_j(\vec{b})]=0$ and which act in the same Hilbert space, that is, which commute with $T_j(\vec{L}_{mn})$. What are the $\vec{a},\vec{b}$ that satisfy these equations? To solve these constraints, it is simple to expand $\vec{a}=\alpha\vec{L}_1+\beta\vec{L}_2$, which is always possible, with α,β real numbers. From the commutator or relative translations with the single-particle translations of primitive lattice vectors, we have, for $j=i$

$$\begin{aligned}0&=[\tilde{T}_i(\vec{a}),T_i(\vec{L}_{mn})]\\&=\prod_{m=1,m\neq i}^{N_e}T_m\left(-\frac{\vec{a}}{N_e}\right)\left[T_i\left(\frac{(N_e-1)\vec{a}}{N_e}\right),T_i(\vec{L}_{mn})\right]\\&=-2i\prod_{m=1,m\neq i}^{N_e}T_m\left(-\frac{\vec{a}}{N_e}\right)T_i\left(\frac{(N_e-1)\vec{a}}{N_e}+\vec{L}_{mn}\right)\\&\quad\times\sin\left[\frac{1}{2l^2}\frac{N_e-1}{N_e}\hat{z}\cdot(\vec{a}\times\vec{L}_{mn})\right].\end{aligned}\tag{20}$$

Hence, we find: $\frac{(N_e-1)}{N_e}\hat{z}\cdot(\vec{a}\times\vec{L}_{mn})=2\pi l^2 r$, where r is an integer. To find the constraints on α,β, we can pick $\vec{L}_{mn}=\vec{L}_1,\vec{L}_2$ to obtain $\frac{(N_e-1)}{N_e}N_\phi\alpha=r$, $\frac{(N_e-1)}{N_e}N_\phi\beta=r$. As we are at filling $N_e/N_\phi=p/q$, we have $(N_e-1)q\alpha=pr$, $(N_e-1)q\beta=pr$, where r is any integer. Also from the commutator or relative translations with the single-particle translations of primitive lattice vectors, for $j\neq i$, we have

$$\begin{aligned}0&=[\tilde{T}_j(\vec{a}),T_i(\vec{L}_{mn})]\\&=T_j\left(\frac{(N_e-1)\vec{a}}{N_e}\right)\prod_{m=1,m\neq i,j}^{N_e}T_m\left(-\frac{\vec{a}}{N_e}\right)\\&\quad\times\left[T_i\left(-\frac{\vec{a}}{N_e}\right),T_i(\vec{L}_{mn})\right]\\&=-2iT_j\left(\frac{(N_e-1)\vec{a}}{N_e}\right)\prod_{m=1,m\neq i,j}^{N_e}T_m\left(-\frac{\vec{a}}{N_e}\right)\\&\quad\times T_i\left(-\frac{\vec{a}}{N_e}+\vec{L}_{mn}\right)\sin\left[\frac{1}{2l^2}\frac{-1}{N_e}\hat{z}\cdot(\vec{a}\times\vec{L}_{mn})\right].\end{aligned}\tag{21}$$

The conditions the above equation gives are $q\alpha=pr$, $q\beta=pr$, where r is any integer, consistent with, but more restrictive than the first set of conditions. We now impose the condition that the $0=[\tilde{T}_i(\vec{a}),\tilde{T}_j(\vec{b})]$. For $i=j$ we have

$$\begin{aligned}\tilde{T}_i(\vec{a})\tilde{T}_i(\vec{b})&=T_i\left(\frac{N_e-1}{N_e}\vec{a}\right)T_i\left(\frac{N_e-1}{N_e}\vec{b}\right)\prod_{l\neq i}^{N_e}T_j\left(-\frac{1}{N_e}\vec{a}\right)T_j\left(-\frac{1}{N_e}\vec{b}\right)\\&=e^{-\frac{i}{2l^2}\hat{z}\cdot(\vec{a}\times\vec{b})(\frac{(N_e-1)^2}{N_e^2}+(N_e-1)\frac{1}{N_e^2})}T_i\left[\frac{N_e-1}{N_e}(\vec{a}+\vec{b})\right]\prod_{l\neq i}^{N_e}T_j\left[-\frac{1}{N_e}(\vec{a}+\vec{b})\right]\\&=e^{-\frac{i}{2l^2}\hat{z}\cdot(\vec{a}\times\vec{b})(\frac{(N_e-1)}{N_e})}T_i\left[\frac{N_e-1}{N_e}(\vec{a}+\vec{b})\right]\prod_{l\neq i}^{N_e}T_l\left[-\frac{1}{N_e}(\vec{a}+\vec{b})\right].\end{aligned}\tag{22}$$

For $\tilde{T}_i(\vec{a})\tilde{T}_i(\vec{b})$ to equal $\tilde{T}_i(\vec{b})\tilde{T}_i(\vec{a})$, we need that $\hat{z}\cdot(\vec{a}\times\vec{b})(\frac{(N_e-1)}{N_e})=2\pi l^2 r$. If $\vec{a}=\alpha\vec{L}_1$, $\vec{b}=\beta\vec{L}_2$ we have $\frac{(N_e-1)}{N_e}\alpha\beta N_\phi=r$ and hence $(N_e-1)q\alpha\beta=pr$ for r some integer. For $i\neq j$ we have

$$\tilde{T}_i(\vec{a})\tilde{T}_j(\vec{b})=T_i\left(\frac{N_e-1}{N_e}\vec{a}-\frac{1}{N_e}\vec{b}\right)T_j\left(\frac{N_e-1}{N_e}\vec{b}-\frac{1}{N_e}\vec{a}\right)\prod_{l\neq i,j}T_l\left[-\frac{1}{N_e}(\vec{a}+\vec{b})\right]e^{-\frac{i}{2l^2}\hat{z}\cdot(\vec{a}\times\vec{b}))[-2(N_e-1)\frac{1}{N_e^2}+(N_e-2)\frac{1}{N_e^2}]}\tag{23}$$

and hence [by taking $\tilde{T}_j(\vec{b})\tilde{T}_i(\vec{a})$ and requiring the vanishing of the commutator], we must set $\hat{z}\cdot(\vec{a}\times\vec{b})[-2(N_e-1)\frac{1}{N_e^2}+(N_e-2)\frac{1}{N_e^2}]=2\pi l^2 r$. If $\vec{a}=\alpha\vec{L}_1,\vec{b}=\beta\vec{L}_2$ we have $q\alpha\beta=pr$.

We now bring the four sets of constraints on α,β together. The conditions for the set a for which the relative translation operators commute between themselves and commute with the $T_i(\vec{L}_{mn})$ are $q\alpha=pr_1$, $q\beta=pr_2$, $q\alpha\beta=pr_3$, $r_1,r_2,r_3\in\mathbb{Z}$. If q is a prime number, then we can show that $\alpha,\beta=p$: We substitute α,β from the first two equations in the third to obtain $pr_1r_2=qr_3$. Since p,q are relatively prime, then $r_3=pr$ and $r_1r_2=qr$, where $r\in\mathbb{Z}$. However, since q is prime, then $r_1r_2=qr$ implies $r_1=qr'$, where $r'\in\mathbb{Z}$ (or vice versa for r_2). We then plug this in $q\alpha=pr_1$ to obtain $\alpha=pr'$ and so α is an integer proportional to p. The smallest value (which gives the largest set of $\vec{a}=\alpha\vec{L}_1$) of this is $\alpha=p$. Then $q\beta=r_3=pr$ and hence $\beta=p$. The set of vectors $\vec{a}$ for which relative translation operators commute with each other *and* with the single-particle momenta is $\vec{a}=p\vec{L}_{mn}$ if q is a prime number. In passing, we note that if q is not a prime, other possibilities arise for the set of maximally commuting relative translations. The simplest case is to assume $q=q_1^2$, that is, q is a perfect square, but same situation occurs whenever q is not prime. Then if we choose $\alpha=\beta=p/q_1$ we have $r_1=r_2=q_1$, $r_3=p$; all integers and hence the relative translation operators commute with themselves and with the one-body translation operators by $\vec{L}_{mn}$. This then gives $\vec{a}=\frac{p}{q_1}\vec{L}_{mn}$. This, however, corresponds to a different choice of resolving the ground-state center-of-mass degeneracy, as is now shown.

The center-of-mass operators $T_{\rm CM}(\vec{L}_{mn}/N_\phi)$ commute with the the $T_i(\vec{L}_{mn})$ but not between themselves (so they cannot all be simultaneously diagonalized):

$$T_{\rm CM}(\vec{L}_{mn}/N_s)T_{\rm CM}(\vec{L}_{m'n'}/N_s) = \prod_{i=1}^{N_e}\{T_i[(\vec{L}_{mn}+\vec{L}_{m'n'})/N_s]e^{-\frac{i}{2l^2}\frac{1}{N_s^2}(mn'-nm')\hat{z}\cdot(\vec{L}_1\times\vec{L}_2)}\}$$
$$= e^{-i\pi\frac{N_e}{N_s}(mn'-nm')}\prod_{i=1}^{N_e}T_i[(\vec{L}_{mn}+\vec{L}_{m'n'})/N_s] = e^{-i\pi\frac{p}{q}(mn'-nm')}\prod_{i=1}^{N_e}T_i[(\vec{L}_{mn}+\vec{L}_{m'n'})/N_s]. \quad (24)$$

As a hint of the q-fold degeneracy of the spectrum, for q a prime number, we see that $T^q_{\rm CM}(\vec{L}_{mn}/N_s)$ commutes with $T_{\rm CM}(\vec{L}_{mn})$. Moreover, if q is not a prime number, and it is, for example, a perfect square $q = q_1^2$, we see that a set of mutually commuting operators is $T^{q_1}_{\rm CM}(\vec{L}_{mn})$.

We now try to diagonalize the maximum commuting set of relative momentum operators $\tilde{T}_i(p\vec{L}_{mn})$ which commute with themselves and also with the $T_i(\vec{L}_{mn})$ operators. We would like to find its eigenvalues, labeled by a 2-momentum $\vec{k}$. Following Haldane, we make the assumption that the many-body state [which is an eigenstate of $\tilde{T}_i(p\vec{L}_{mn})$] experiences, when acted on by $\sum_{i=1}^{N_e}\exp(i\vec{Q}\cdot\vec{r}_i)$, an increase in its momentum by $\vec{Q}$, as long as $\vec{Q}$ is a reciprocal lattice momentum $\exp(i\vec{Q}\cdot\vec{L}_{mn}) = 1$. In other words, let the eigenstates of $\tilde{T}_i(p\vec{L}_{mn})$ be $|\psi(\vec{k})\rangle$, with eigenvalue $\lambda_{\vec{k}}$,

$$\tilde{T}_i(p\vec{L}_{mn})|\psi(\vec{k})\rangle = \lambda_{\vec{k}}|\psi(\vec{k})\rangle, \quad \sum_i e^{i\vec{Q}\cdot\vec{r}_i}|\psi(\vec{k})\rangle = |\psi(\vec{k}+\vec{Q})\rangle. \quad (25)$$

By applying $\tilde{T}_i(p\vec{L}_{mn})$ on the $\sum_i e^{i\vec{Q}\cdot\vec{r}_i}|\psi(\vec{k})\rangle$ we obtain

$$\lambda_{\vec{k}+\vec{Q}}|\psi(\vec{k}+\vec{Q})\rangle = \tilde{T}_i(p\vec{L}_{mn})\sum_j^{N_e}e^{i\vec{Q}\cdot\vec{r}_j}|\psi(\vec{k})\rangle = T_i\left(\frac{N_e-1}{N_e}p\vec{L}_{mn}\right)\prod_{l\neq i}T_l\left(-\frac{p\vec{L}_{mn}}{N_e}\right)\left(e^{i\vec{Q}\cdot\vec{r}_i}+\sum_{j\neq i}^{N_e}e^{i\vec{Q}\cdot\vec{r}_j}\right)|\psi(\vec{k})\rangle$$
$$= \left(e^{-i\vec{Q}\frac{p\vec{L}_{mn}}{N_e}}\sum_{l\neq i}^{N_e}e^{i\vec{Q}\cdot\vec{r}_l}+e^{i\vec{Q}\frac{N_e-1}{N_e}p\vec{L}_{mn}}e^{i\vec{Q}\cdot\vec{r}_i}\right)\tilde{T}_i(p\vec{L}_{mn})|\psi(\vec{k})\rangle$$
$$= e^{-i\frac{p}{N_e}\vec{Q}\cdot\vec{L}_{mn}}\sum_j^{N_e}e^{i\vec{Q}\cdot\vec{r}_j}\lambda_{\vec{k}}|\psi(\vec{k})\rangle = e^{-i\frac{p}{N_e}\vec{Q}\cdot\vec{L}_{mn}}\lambda_{\vec{k}}|\psi(\vec{k}+\vec{Q})\rangle. \quad (26)$$

We have then $\lambda_{\vec{k}+\vec{Q}} = \lambda_{\vec{k}}e^{-i\frac{p}{N_e}\vec{Q}\cdot\vec{L}_{mn}}$ and hence $\lambda_{\vec{k}} = De^{-i\frac{p}{N_e}\vec{k}\cdot\vec{L}_{mn}}$. D can only be a phase independent on $\vec{k}$. The constant D can be found by requiring that the $\vec{k}=0$ state remains invariant under all translations:

$$D|\psi(\vec{k}=0)\rangle = \tilde{T}_i(p\vec{L}_1)|\psi(\vec{k}=0)\rangle = \tilde{T}_i(-p\vec{L}_2)|\psi(\vec{k}=0)\rangle = \tilde{T}_i(p\vec{L}_2-p\vec{L}_1)|\psi(\vec{k}=0)\rangle. \quad (27)$$

However, the last term $\tilde{T}_i(p\vec{L}_2-p\vec{L}_1)$ can be reexpressed in terms of the product of the translation operators of $p\vec{L}_2$ and $p\vec{L}_1$. We have

$$\tilde{T}_i(p\vec{L}_2)\tilde{T}_i(-p\vec{L}_1) = T_i\left(\frac{N_e-1}{N_e}p\vec{L}_2\right)T_i\left(-\frac{N_e-1}{N_e}p\vec{L}_1\right)\prod_{l\neq i}T_l\left(-\frac{1}{N_e}p\vec{L}_2\right)T_l\left(\frac{1}{N_e}p\vec{L}_1\right)$$
$$= T_i\left[\frac{N_e-1}{N_e}p(\vec{L}_2-\vec{L}_1)\right]\prod_{l\neq i}T_l\left[-\frac{1}{N_e}p(\vec{L}_2-\vec{L}_1)\right]e^{\frac{i}{2l^2}\frac{(N_e-1)^2}{N_e^2}p^2\hat{z}\cdot(\vec{L}_2\times\vec{L}_1)}e^{\frac{i}{2l^2}\frac{N_e-1}{N_e^2}p^2\hat{z}\cdot(\vec{L}_2\times\vec{L}_1)}$$
$$= \tilde{T}_i(p\vec{L}_2-p\vec{L}_1)e^{\frac{i}{2l^2}\frac{N_e-1}{N_e}p^2(-2\pi l^2N_s)} = \tilde{T}_i(p\vec{L}_2-p\vec{L}_1)e^{\frac{i}{2l^2}\frac{N_e-1}{N_e}p^2(-2\pi l^2N_s)} = \tilde{T}_i(p\vec{L}_2-p\vec{L}_1)e^{-i(N_e-1)pq\pi}. \quad (28)$$

Thisyields the equation $D|\psi(\vec{k}=0)\rangle = D^2e^{i(N_e-1)pq\pi}|\psi(\vec{k}=0)\rangle$, which gives $D=(-1)^{(N_e-1)pq}$. After establishing the constant D, we would like to now find the possible values that $\vec{k}$ can take. We remark that $N_e = pN$ and $N_\phi = qN$ and, hence,

$$\tilde{T}_i(p\vec{L}_{mn}) = T_i\left(\frac{N_e-1}{N}\vec{L}_{mn}\right)\prod_{l\neq i}T_l\left(-\frac{\vec{L}_{mn}}{N}\right). \quad (29)$$

We know that $T_i(\vec{L}_{mn})$ has fixed eigenvalue θ_{mn} (which for identical particles does not depend on i). This means that the Nth power of the relative $\tilde{T}_i(p\vec{L}_{mn})$ operator has a fixed eigenvalue:

$$\tilde{T}_i(p\vec{L}_{mn})^N = T_i[(N_e-1)\vec{L}_{mn}]\prod_{l\neq i}^{N_e}T_l(-\vec{L}_{mn})$$
$$= e^{i\theta_{mn}(N_e-1)}\prod_{l\neq i}^{N_e}e^{-i\theta_{mn}} = 1 = D^Ne^{-i\vec{k}\cdot\vec{L}_{mn}}. \quad (30)$$

Having determined the constant D, we have $D^N = (-1)^{qN_e(N_e-1)} = 1$. Hence, $e^{-i\vec{k}\cdot\vec{L}_{mn}} = 1$, and we have as solutions $\vec{k}\cdot\vec{L}_1 = 2\pi i$, $\vec{k}\cdot\vec{L}_2 = 2\pi j$, $i,j \in Z$. We now must ask how many of these solutions represent unique eigenvalues of $\tilde{T}_i(p\vec{L}_{mn})$. Its eigenvalues are $(-1)^{pq(N_e-1)}\exp(-i\vec{k}\cdot\vec{L}_{mn}/N)$, and are different for $\vec{k}\cdot\vec{L}_1 = 2\pi i$, $\vec{k}\cdot\vec{L}_2 = 2\pi j$, $i,j \in [1,\ldots,N]$. Hence, the BZ of the relative translation operators is made up of $N\times N$ values of the momentum. An alternative way of presenting the resulting momenta is to say that the eigenvalues of the relative momentum $\tilde{T}_i(p\vec{L}_{mn})$ are $e^{-i\vec{k}\cdot\vec{L}_{mn}/N}$, with $\vec{k}l = \sqrt{\frac{2\pi}{N_s\lambda}}[s-s_0,\lambda(t-t_0)]$, where $s,t = 1,\ldots,N$ and $\lambda = L_x/L_y$ is the aspect ratio, while the s_0,t_0 are the quantum numbers belonging to zero momentum: $\exp(2\pi i s_0/N) = \exp(2\pi t_0/N) = (-1)^{pq(N_e-1)}$. This exhausts our discussion of the relative translation operators.

Having fixed θ_1,θ_2,k, we now ask if there are any other degeneracies. The answer is yes. Physically, this is because θ_1,θ_2 define the single-particle Hilbert space while k is the principal symmetry quantum number of the relative wave function $|\psi_{\rm rel}\rangle$. Left untouched so far is the center-of-mass translational symmetry of the problem, or the center-of-mass wave function $|\psi_{\rm CM}\rangle$. In principle, we have diagonalized only the $\tilde{T}_i(p\vec{L}_{mn})$ but there are missing center-of-mass operators, $T_{\rm CM}(\vec{L}_{mn}/N_s)$, which also commute with the $T_i(\vec{L}_{mn})$ operators and keep us in the same Hilbert space; also, any center-of-mass translation operator commutes with the relative translation operator, and hence we are well on our way toward finding other commuting operators. *However, crucially, two center-of-mass translations $T_{\rm CM}(\vec{L}_{mn}/N_s)$ and $T_{\rm CM}(\vec{L}_{m'n'}/N_s)$ do not commute with each other* and hence they cannot be simultaneously diagonalized. We hence must find the maximum set of $T_{\rm CM}(\vec{L}_{mn}/N_s)$ that can be diagonalized, which, per the above, is equal to the maximally commuting set of $T_{\rm CM}(\vec{L}_{mn}/N_s)$. We can find out how many $T_{\rm CM}(\vec{L}_{mn}/N_s)$ are self-commuting by either brute-force calculation or by a smart argument. We start with the brute-force calculation of the commutator:

$$\begin{aligned}\left[T_{\rm CM}\left(\frac{\vec{L}_{mn}}{N_s}\right),T_{\rm CM}\left(\frac{\vec{L}_{m'n'}}{N_s}\right)\right]&\\ = e^{-\frac{i}{2l^2}\frac{\hat{z}\cdot(\vec{L}_{mn}\times\vec{L}_{m'n'})}{N_s^2}N_e}\prod_{i=1}^{N_e}T_i\left(\frac{\vec{L}_{mn}+\vec{L}_{m'n'}}{N_s}\right)&\\ = e^{-i\pi\frac{p}{q}(mn'-nm')}\prod_{i=1}^{N_e}T_i\left(\frac{\vec{L}_{mn}+\vec{L}_{m'n'}}{N_s}\right),&\end{aligned}\tag{31}$$

which vanishes if and only if $(mn'-nm')/q \in \mathbb{Z}$. Hence, there are q values possible. If we require $|\psi_{\rm CM}\rangle$ to be an eigenstate of $T_{\rm CM}(L^0/N_s)$, where L^0 is some particular primitive translation, the set of all center-of-mass translations that commute with $T_{\rm CM}(\vec{L}^0/N_s)$ is given by $\{T_{\rm CM}[(q\vec{L}_{mn}+r\vec{L}^0)/N_s]\}$, with $r = 0,1,\ldots,q-1$. Indeed, the commutator

$$\{T_{\rm CM}[(q\vec{L}_{mn}+r\vec{L}^0)/N_s],T_{\rm CM}[(q\vec{L}_{m'n'}+r\vec{L}^0)/N_s]\} = 0.\tag{32}$$

As Haldane mentions,[19] this is only one of the few resolutions of the center of mass degeneracy. The smart and quick argument which reveals the q-fold degeneracy is the following: We know that

$$T_i(p\vec{L}_{mn}) = T_{\rm CM}(p\vec{L}_{mn}/N_e)\tilde{T}_i(p\vec{L}_{mn})\tag{33}$$

and hence the eigenvalue of

$$[T_{\rm CM}(\vec{L}_{mn}/N_s)]^q = T_{\rm CM}(p\vec{L}_{mn}/N_e) = T_i(p\vec{L}_{mn})\tilde{T}_i(-p\vec{L}_{mn})\tag{34}$$

is fixed once we have diagonalized θ_1,θ_2,k to be $(-1)^{pq(N_e-1)}\exp(ip\theta_{mn})\exp(iqk\cdot\vec{L}_{mn}/N_s)$. Since only the qth power of the eigenvalue is fixed, we see that there must be q center-of-mass operators (of different eigenvalues). If the eigenvalue of $T_{\rm CM}(\vec{L}^0/N_s)$ is λ, then the eigenvalues of the set of maximally commuting center-of-mass operators $\{T_{\rm CM}[(q\vec{L}_{mn}+r\vec{L}^0)/N_s]\}$ with $r = 0,1,\ldots,q-1$ have eigenvalues $\lambda^r(-1)^{pqr(N_e-1)}\exp(ip\theta_{mn})\exp(iqk\cdot\vec{L}_{mn}/N_s)$. This completes the many-body theoretical symmetry analysis of the spectrum of FQH states. The section so far did not contain new material, although we believe and hope that the detailed and expanded description of the calculations present in Ref. 19 is useful to the reader.

C. Building the Hilbert space

On the torus, each Landau level has an identical number of states that it can accommodate. The operator for an electron at position (x,y) is $\psi(x,y) = \sum_{m,j}\phi_{m,j}(x,y)c_{m,j}$, where $c_{m,j}$ is the annihilation operator of an electron of momentum j in the mth Landau level, and the $\phi_{m,j}$ are the single-particle orbitals:

$$\begin{aligned}\phi_{m,j}(x,y) = \sum_{k\in\mathbb{Z}} e^{\frac{2\pi}{L_y}(j+kN_\phi)(x+iy)}e^{-\frac{x^2}{2l^2}}e^{-\frac{1}{2}(\frac{2\pi l}{L_y})^2(j+kN_\phi)^2}&\\ \times H_m\left[\frac{2\pi l}{L_y}(j+kN_\phi)-\frac{x}{l}\right].&\end{aligned}\tag{35}$$

H_m is the Hermite polynomial. In the above, we have picked the Landau gauge $\vec{A} = Bx\hat{y}$. While the single-particle orbitals given above are not normalized, it is crucial to notice that the normalization factor depends only on the Landau level index m and not on the orbital momentum j. This is a feature of the torus geometry; on the sphere the single-particle orbitals depend on the angular momentum quantum number. For the lowest Landau level, to which we particularize, $H_0 = 1$. The translational properties of the single-particle orbitals (for a rectangular lattice $\vec{L}_1 = L_x\hat{x},\vec{L}_2 = L_y\hat{y}$) are trivially obtained:

$$\begin{aligned}\phi_{m,j}(x,y+L_y) &= \phi_{m,j}(x,y),\\ \phi_{m,j}(x+L_x,y) &= e^{i\frac{2\pi}{L_y}N_\phi y}\phi_{m,j}(x,y).\end{aligned}\tag{36}$$

In order to obtain the action of the relative translation operators on the many-body states, we note the translational properties under translations by $(N_e-1)p\vec{L}_{mn}/N_e$ and by $-p\vec{L}_{mn}/N_e$:

$$\begin{aligned}\phi_{m,j}\left(x,y+\frac{N_e-1}{N_e}pL_y\right) = \phi_{m,j}\left(x,y-\frac{1}{N_e}pnL_y\right)&\\ = e^{-i\frac{2\pi j}{N}}\phi_{m,j}(x,y),&\end{aligned}\tag{37}$$

$$\phi_{m,j}\left(x+\frac{N_e-1}{N_e}pL_x,y\right)=e^{i\frac{2\pi}{L_y}q(N_e-1)y}\phi_{m,j+q}(x,y),$$
$$\phi_{m,j}\left(x-\frac{1}{N_e}pL_x,y\right)=e^{-i\frac{2\pi}{L_y}qy}\phi_{m,j+q}(x,y). \quad (38)$$

In the Landau gauge used, the guiding center translation operator $T(\vec{L})$ is related to the usual translation operator $t(\vec{L})=\exp \vec{L}\cdot\vec{\nabla}$ by $T(\vec{L})=\exp[\frac{i}{l^2}(L_x y+\frac{1}{2}L_xL_y)]t(\vec{L})$. On a one-body state $T(\vec{L})\,|m,j\rangle=\iint dxdy T(\vec{L})\,|x,y\rangle\,\langle x,y\,|m,j\rangle=\iint dxdy\exp\{\frac{i}{l^2}[L_x(y+L_y)+\frac{1}{2}L_xL_y]|x+L_x,y+L_y\rangle\}\langle x,y\,|m,j\rangle$, where $\langle x,y\,|m,j\rangle=\phi_{m,j}(x,y)$. By switching variables in the integral, we have $T(\vec{L})\,|m,j\rangle=\iint dxdy\exp[\frac{i}{l^2}(L_xy+\frac{1}{2}L_xL_y)\,|x,y\rangle]\langle x-L_x,y-L_y\,|m,j\rangle$. Using the properties of Eqs. (37) and (38), we can prove the following:

$$\tilde{T}_i(pL_y\hat{y})|j_1,\ldots,j_{N_e}\rangle=e^{i\frac{2\pi}{N}\sum_{i=1}^{N_e}j_i}|j_1,\ldots,j_{N_e}\rangle. \quad (39)$$

This was possible because there is no L_x in the $\vec{L}=pL_y\hat{y}$ translation, and hence the factor $\exp[\frac{i}{l^2}(L_xy+\frac{1}{2}L_xL_y)]=1$. The relative translation operator by $pL_x\hat{x}$, $\tilde{T}_i(pL_x\hat{x})$ has the factor $\exp(\frac{i}{l^2}\frac{N_e-1}{N_e}pL_xy)=\exp[i\frac{2\pi}{L_y}q(N_e-1)y_i]$ if it acts on the particle i in the single-particle decomposition, which cancels the factor $\exp[-i\frac{2\pi}{L_y}q(N_e-1)y_i]$ present in $\langle x_i-\frac{N_e-1}{N_e}pL_x,y_i\,|m,j\rangle$. Similarly, $\tilde{T}_i(pL_x\hat{x})$ there contains operators $T_j(-pL_x\hat{x}/N_e)$. These give a factor $\exp(-\frac{i}{l^2}\frac{1}{N_e}pL_xy_j)=\exp(-i\frac{2\pi}{L_y}qy_j)$ which cancel the factor $\exp(i\frac{2\pi}{L_y}qy_j)$ arising from $\langle x_j-\frac{-1}{N_e}pL_x,y_j\,|m,j\rangle$. We hence obtain

$$\tilde{T}_i(pL_x\hat{x})|j_1,\ldots,j_{N_e}\rangle=|j_1+q,\ldots,j_{N_e}+q\rangle. \quad (40)$$

We hence found that (in the Landau gauge), the many-body Hilbert space vectors $\left|j_1,\ldots,j_{N_e}\right\rangle$ is an eigenstate of $\tilde{T}_i(pL_y\hat{y})$ with eigenvalue $e^{i\frac{2\pi}{N}\sum_{i=1}^{N_e}j_i}$ dependent on the total momentum $\sum_{i=1}^{N_e}j_1(\mathrm{mod}\,N)$. Due to the denominator N, the momentum is defined only by $\mathrm{mod}\,N$, which is an explicit way of seeing that the relative momentum BZ is made out of N k_y momenta. Note, however, and this is *essential*, that this does *not* imply that all states with identical $\sum_{i=1}^{N_e}j_i(\mathrm{mod}\,N)$ belong to the same Hilbert space. In fact, only states with all $\sum_{i=1}^{N_e}j_i(\mathrm{mod}\,N_\phi)$ belong to the same Hilbert space. The construction of relative translational symmetry-sorted Hilbert space proceeds as follows: First, write all possible states $|j_1,\ldots,j_{N_e}\rangle$ with no constraint other than no double occupancy of orbitals in the case of fermions. Now sort the Hilbert space into different sectors given by the constraint that each sector contains terms with identical $\sum_{i=1}^{N_e}j_i(\mathrm{mod}\,N_\phi)$. No two states having different $\sum_{i=1}^{N_e}j_i(\mathrm{mod}\,N_\phi)$ can be coupled by a momentum-conserving Hamiltonian. Since $N_\Phi=qN$, there will, in general, be several more sectors, with different $\sum_{i=1}^{N_e}j_i(\mathrm{mod}\,N_\phi)$, which have the same $\sum_{i=1}^{N_e}j_i(\mathrm{mod}\,N)$. It is hence a mistake to first sort the Hilbert space first by sectors with identical $\sum_{i=1}^{N_e}j_i(\mathrm{mod}\,N)$: This will result in a much larger number of free-many-body states per sector, because the states have yet to be sorted by $\sum_{i=1}^{N_e}j_i(\mathrm{mod}\,N_\Phi)$. Once we have sorted the states by $\sum_{i=1}^{N_e}j_i(\mathrm{mod}\,N_\phi)$, for the elements in one sector (which has a momentum $\exp(-ik_yL_y/N)=\exp(i2\pi\sum_{i=1}^{N_e}j_i/N)\exp[i\pi pq(N_e-1)]$) we must implement the translational symmetry in the other direction. As the translation operator $\tilde{T}_i(pL_x\hat{x})$ takes $|j_1,\ldots,j_{N_e}\rangle$ into $|j_1+q,\ldots,j_{N_e}+q\rangle$ (which crucially, has a the identical $\sum_{i=1}^{N_e}(j_i+q)(\mathrm{mod}\,N_\phi)=(qN_e+\sum_{i=1}^{N_e}j_i)(\mathrm{mod}\,N_\phi)=\sum_{i=1}^{N_e}j_i(\mathrm{mod}\,N_\phi)$, and same thing with N_ϕ replaced by N, so k_y remains unchanged), we must form the orbits of this operator. This operation goes as follows: For every element of the set $|j_1,\ldots,j_{N_e}\rangle$ form all the elements $|j_1+qk,\ldots,j_{N_e}+qk\rangle$ with $k\in\mathbb{Z}$. These elements form the orbit of $\tilde{T}_i(pL_x\hat{x})$. Let the number of elements in an orbit be Z. We can form eigenstates of the $\tilde{T}_i(pL_x\hat{x})$ by taking combinations of the states in an orbit:

$$|k_x,k_y\rangle=\sum_{k=0}^{Z}e^{i\frac{2\pi n}{N}k}|j_1+qk,\ldots,j_{N_e}+qk\rangle, \quad (41)$$

where n is an integer. The k_y momentum of these states has been already established by the equation $\exp(-ik_yL_y/N)=\exp(i2\pi\sum_{i=1}^{N_e}j_i/N)\exp[i\pi pq(N_e-1)]$. To establish the k_x momentum, we note that

$$\tilde{T}_i(pL_x\hat{x})|k_x,k_y\rangle=e^{i\frac{2\pi n}{N}}|k_x,k_y\rangle$$
$$=(-1)^{pq(N_e-1)}\exp(-ik_xL_x/N)|k_x,k_y\rangle \quad (42)$$

and, hence, $\exp(-ik_xL_x/N)=\exp(i2\pi n/N)\exp[i\pi pq(N_e-1)]$, where $n\in[0,\ldots,N-1]$ is an integer. These are the basis states explicitly translationally invariant with the relative translation operator. They allow a large simplification of numerical computation and explain the degeneracies observed in the spectrum of any translationally invariant Hamiltonian. We come back in more detail to the explicit construction of a translationally invariant Hilbert space in the Sec. III.

D. The density algebra in the lowest Landau level

The results above can be put in an equivalent form when written in terms of the projected density algebra. In a similar way to how one defined the guiding center momentum $K_\alpha=\Pi_\alpha-\frac{\hbar}{l^2}(\hat{z}\times\vec{r})_\alpha$, a guiding center coordinate R_α (one-body operator) can be defined

$$R_\alpha=r_\alpha-\frac{l^2}{\hbar}(\vec{\Pi}\times\hat{z})_\alpha,\quad \vec{R}=\frac{l^2}{\hbar}\hat{z}\times\vec{K}, \quad (43)$$

where r is the position of the particle. The guiding center coordinate is then related to the guiding center position and one can obtain the similar commutations: $[\Pi_\alpha,R_\beta]=0$, $[R_\alpha,R_\beta]=il^2\epsilon_{\alpha\beta z}$. We cannot build a guiding center density operator:

$$\rho(\vec{q})=e^{i\vec{q}\cdot\vec{R}}. \quad (44)$$

It is known that this operator has several interesting properties. First, it satisfies the GMP algebra:

$$\rho(\vec{q})\rho(\vec{q}')=\rho(\vec{q}+\vec{q}')e^{-\frac{i}{2}l^2(\vec{q}\times\vec{q}')\cdot\hat{z}}, \quad (45)$$

which is not surprising as it is just a restatement of the guiding center translation operator:

$$T(\vec{L}) = \rho\left(\frac{\hat{z}\times\vec{L}}{l^2}\right). \quad (46)$$

The relation between the translation operators and densities means that *all* the many-body translation operators obtained in the previous section can be expressed in terms of the density operators. If we define the two fundamental lattice momenta $\vec{q}_1 = 2\pi\vec{L}_2/\mathcal{A}$, $\vec{q}_2 = -2\pi\vec{L}_1/\mathcal{A}$, where $\mathcal{A}$ is the area of the BZ $\mathcal{A} = 2\pi l^2 N_\phi$, we obtain $T(\vec{L}_{mn}) = (\rho(\vec{q}_{nm}))^{N_\phi}$ with $q_{mn} = m\vec{q}_1 + n\vec{q}_2$, and $[(\rho(\vec{q}_{nm}))^{N_\phi}, H] = 0$. From here on, one can just copy the many-body formulation of the translation operators to obtain it in terms of the guiding center densities and define a center-of-mass density $\bar{\rho}(\vec{q}_{nm}) = \prod_{i=1}^{N_e}\rho_i(\vec{q}_{nm})$ and a set of self-commuting relative density operators $\tilde{\rho}_i(pN_\phi\vec{q}_{nm}) = \rho_i[(N_e-1)pN_\phi\vec{q}_{nm}/N_e]\prod_{j\neq i}^{N_e}\rho_j(-pN_\phi\vec{q}_{nm}/N_e)$, which can be simultaneously diagonalized to obtain the relative momentum quantum numbers, an identical copy of the situation encountered in the translation operator example.

It is crucial to understand how the guiding center density relates to the usual density operator $\rho_0(\vec{q}) = \exp(i\vec{q}\cdot\vec{r})$. It is easy to prove that, up to a factor, the guiding center density equals the projection of the usual density operator into the lowest Landau level:

$$Pe^{i\vec{q}\cdot\vec{r}}P = e^{-\frac{q^2l^2}{4}}\rho(\vec{q}). \quad (47)$$

In other words, the guiding center density is the projection of the usual density into the lowest band of the Landau level insulator. Let us recapitulate the bidding. The many-body translational symmetries can be expressed in terms of a set of many-body density operators that obey a GMP algebra and who are the projection of the regular density operators in the lowest band of the insulator.

III. COUNTING OF ZERO MODES FOR THE READ-REZAYI AND OTHER MODEL STATES (AND QUASIHOLES) PER MOMENTUM SECTOR ON THE TORUS

In this section, we present a procedure which allows for the computation of the number of zero modes (ground states and quasiholes) of many model FQH states resolved per each k_x,k_y momentum sector of the relative translational operators $\tilde{T}_i(pL_x\hat{x}), \tilde{T}_i(pL_y\hat{y})$. We aim to obtain this counting *without* diagonalizing the Hamiltonians for which these model states are exact zero modes. We aim to give a combinatoric procedure for counting the states that is valid and can be performed for any number of particles. All states whose quasihole counting satisfied a generalized Pauli principle in orbital space are amenable to our construction. In a later section, we use this counting and the one numerically obtained from the FCI to check the emergent symmetry proposed in the FCI.

We work with a system of N_ϕ orbitals. If that system was the sphere manifold, the problem of counting the zero modes of certain pseudopotential Hamiltonians can be related to the problem of counting partitions satisfying certain conditions. The same conditions, subject to another periodicity constraint, are valid on the torus. We now state and justify these conditions, which have been obtained in previous studies.[21–29] Fermionic/bosonic many-body wave functions of N_e particles on any manifold can be expressed as linear combinations of Fock states in the occupation number basis of the single-particle orbitals. Each Fock state $|\lambda\rangle$ can be labeled either by the list of occupied orbitals, λ, or by the occupation number configuration, $n(\lambda)$. $\lambda = [\lambda_1,\lambda_2,\ldots,\lambda_{N_e}]$ is an ordered partition of (the z angular momentum $L_z^{\rm tot}$ on the sphere and) the one-dimensional momentum $K = \sum_{i=1}^{N_e}\lambda_i (\mathrm{mod}\, N_\phi)$ on the torus into N_e parts and each orbital with index λ_j is occupied in the Fock state. We number the orbitals on the torus from 0 to $N_\phi - 1$, and hence each λ_i belongs to this interval. By definition, $\lambda_i \geqslant \lambda_j$ if $i < j$, and reordering of the basis acquires the appropriate number of negative signs depending on whether the state is bosonic or fermionic. $n(\lambda)$ is the occupation number configuration. It is defined as $n(\lambda) = \{n_j(\lambda), j = 0,\ldots N_\phi\}$, where $n_j(\lambda)$ is the occupation number of the single-particle orbital with (angular) $1-D$ momentum j. In the un-normalized basis in the lowest Landau level on the torus,

$$\langle z_1,\ldots,z_N|\lambda\rangle = S\big[\phi_{0,\lambda_1}(z_1)\cdot\ldots\cdot\phi_{0,\lambda_N}(z_N)\big], \quad (48)$$

where S is the process of symmetrization/antisymmetrization over all indices i,j such that $\lambda_i \neq \lambda_j$. In this section, we repeatedly use special kinds of partition: the so-called (k,r)-admissible partition. For bosons, a (k,r)-admissible partition labels a configuration whose occupation configuration has no more than k particles in r consecutive orbitals. For fermions, a (k,r)-admissible partition labels a configuration whose occupation number has no more than k particles in $k+r$ consecutive orbitals *and* not more than two particles in two consecutive orbitals. For example, [2,2,0,0] is a (2,2)-admissible bosonic partition on the torus of $N_\phi = 4$, while 2,1,0,0 is not. On the torus, due to its periodicity (the orbital of one-dimensional momentum 0 is identified with the one of momentum N_ϕ) [2,2,0,0] is not a (2,2)-admissible partition on the torus of $N_\phi = 3$, as depicted in Fig. 1. For obvious reasons, we call these admissibility rules generalized Pauli principles. Partitions satisfying Pauli generalized principles as the (k,r) one above, or other more complex ones play a prominent role in the physics of the FQH as it was proved that they count the Hilbert space of the quasiholes of many model FQH liquids. The number of $(k,2)$-admissible partitions count the number of quasiholes of the $\mathbb{Z}_k$ RR state, while the generic (k,r) case counts the number of Jack polynomials states. On the sphere, other concepts such as squeezing, etc., are important, but they are not on the torus and we do not discuss

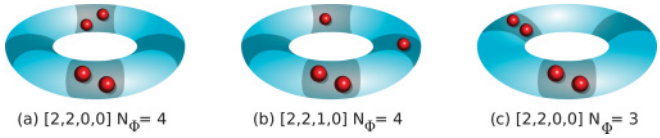

FIG. 1. (Color online) A schematic view of the partitions on the torus geometry. The shaded regions are the orbitals [four for panels (a) and (b), three for panel (c)]. Among the three examples, only situation (a) corresponds to a (2,2)-admissible partition on the torus. On the sphere geometry, both (a) and (c) would be (2,2)-admissible partitions.

them further, referring the reader to the existing literature.[30] On the sphere and on the torus, the bosonic RR sequence at filling $\nu = k/2$ here (see Sec. III for other model states), are the unique, highest-density zero-mode wave functions of $(k+1)$-body pseudopotential Hamiltonians.[31] Recent work[21] has shown the RR bosonic wave functions ψ to be Jack polynomials $J^{\alpha}_{\lambda_0}$ indexed by a parameter $\alpha = -(k+1)$ and the densest possible $(k,2)$-admissible "root" configuration[32] $n(\lambda_0) = \{k0k0k0\cdots k0k\}$. On the torus, no extension of the Jack polynomials exist, but the correspondence between zero mode and partition counting is still valid. One can imagine it does, as the admissible partitions implement a generalized Pauli exclusion statistics, which should be independent of the manifold on which the state resides. On the torus, at filling $k/2$, $N_\phi = 2N_e/k$ for the ground-state and bosonic $(k,2)$-admissible partitions, we obtain the correct degeneracy ($k+1$ for the $\mathbb{Z}_k$ RR ground states on the torus) by just counting the occupation number configurations with no more than k particles in two consecutive orbitals $[k\ 0\ k\ 0,\ldots,k\ 0]$, $[k-1\ 1\ k-1\ 1,\ldots,k-1\ 1]$, $[k-2\ 2\ k-2\ 2,\ldots,k-2\ 2]$, and so on until $[0\ k\ 0\ k,\ldots,0\ k]$. Quasihole counting proceeds identically. Counting states through partitions in this way is usually referred to as the "thin"-torus limit, although we stress that this counting also applies for the sphere (where it can be analytically proved through the Jack-polynomial mapping), as well as for the finite-size torus.

The counting of quasiholes for the Jack polynomial states proceeds as follows. First, in the one-dimensional momentum on the torus, write all the (k,r) partitions ($r = 2$ gives the RR series) $\lambda = [\lambda_1,\ldots,\lambda_{N_e}]$ possible on the torus (remembering that the torus is periodic). Their number is the *total* number of the quasihole states for that flux. We now aim to resolve the partitions by assuming they represent states and check their properties under the relative translation operators. It is trivial to first resolve k_y. To obtain all the states (unresolved in k_x) at a certain k_y we sort the partitions based on the values of $\sum_{i=1}^{N_e}\lambda_i (\mathrm{mod}\, N_\phi)$. Partitions with the same $\sum_{i=1}^{N_e}\lambda_i (\mathrm{mod}\, N_\phi)$ belong to the same k_y, whose value given by $\exp(-ik_yL_y/N) = \exp[i2\pi\sum_{i=1}^{N_e}\lambda_i/N)\exp(i\pi pq(N_e-1)]$. Call such a set of partitions $\{\lambda^{k_y}\}$. We now must implement the translational symmetry in the x direction with momentum k_x, which we do as in the previous section. From all the partitions $\{\lambda^{k_y}\}$ we again form the orbits by taking all partitions $[\lambda_1+qs,\ldots,\lambda_{N_e}+qs]$, forming the orbit of number of elements Z and form the states $\sum_{s=0}^{Z}\exp(i2\pi ns/N)[\lambda_1+qs,\ldots,\lambda_{N_e}+qs]$ with momentum $\exp(-ik_xL_x/N) = \exp(i2\pi n/N)\exp[i\pi pq(N_e-1)]$. Several important things must be taken into account: In the elements of one orbit, $[\lambda_1+qs,\ldots,\lambda_{N_e}+qs]$, one needs to bring them to the same form of *decreasing* elements. Note that this is not trivial as λ_i+qs is defined as mod N_ϕ and that it could involve sign changes for fermions. Also, for some n's the linear combination of the orbit's partitions might not exist, as some states make up single orbits. We see this in the example below. For other orbits, the number of elements might be smaller than N, in which case again not all k_x momenta can be present. By building the states $|k_x,k_y\rangle$ one can clearly see which momenta are missing. After momentum resolving, we can easily count the number of states in each k_x,k_y sector. Note that while this procedure is constructive (we do not have a theoretical expression for the number of quasiholes per sector, but only a way to construct them), it is an analytic map from a series of admissible partitions in one dimension to a two-dimensional relative momentum BZ.

A complete understanding of how the counting of quasiholes per sector works comes from working out an example. We try to resolve the counting of quasihole states of a $\nu = 1/3$ Laughlin state of two electrons $N_e = 2$ on a torus of $N_\phi = 12$. The quasihole states are the zero modes of the Laughlin quasiholes. Per our analysis above, the spectrum of any translationally invariant Hamiltonian has a (note $N_e/N_\phi = 1/6$ is the filling of the system; the degeneracy comes from it, but we are looking at the quasiholes of the $\nu = 1/3$ Laughlin state, and the counting will reflect that) sixfold degeneracy. We aim to show that the counting of zero modes satisfies this center-of-mass degeneracy. Note that the value of N_e/N_ϕ fixes the degeneracy while the specified FQH state whose quasiholes we try to find $\nu = 1/3$ fixes the Pauli principle responsible for the counting. To start, we write *all* the (1,3)-admissible partitions in $N_\phi = 12$ orbitals of $N_e = 2$ particles. There are 42 such configurations and they are given in Table I. Since $N_e/N_\phi = 1/6$, by our theory, the spectrum should be sixfold center-of-mass degenerate. The nondegenerate states should be resolved by k_y and k_x relative translation momenta, which each take $GCD(N_e,N_\phi) = 2$ values $0,2\pi/L_y$ and $0,2\pi/L_x$. Per our procedure, we first sort the state into ones with values $\sum_{i=1}^{N_e}\lambda_i (\mathrm{mod}\, N_\phi)$. Table II presents the partitions sorted in such way (they can obviously also be read from the fifth column of Table I).

Notice that the $\sum_{\lambda_i}\mathrm{mod}\, N = 0$ sector (which is the equivalent of the $k_y = 0$ sector, as $(-1)^{pq(N_e-1)} = 1$ has three elements while the $\sum_{\lambda_i}\mathrm{mod}\, N = 1$ sector (the $k_y = 2\pi/L_y$ sector) has four elements. Notice how the counting of each of the $k_y = 0,\pi/L_y$ sectors is $q = 6$-fold degenerate, as the theoretical symmetry analysis mentions. We now would like to implement the x translational symmetry to find the counting of Laughlin quasiholes per momentum sector. The same result is obtained no matter which of the sixfold degenerate sectors we pick.

We first look at $k_y = 0$ sector with the states mapped by the partitions [8,4],[9,3],[10,2]. To form the orbits we must look at all elements $[\lambda_1+qs,\lambda_2+qs] = [\lambda_1+6s,\lambda_2+6s]$. The orbit of [8,4] contains $[14,10] \equiv [2,10]$ (and obviously the orbit of [10,2] contains $[16,8] \equiv [4,8]$). Hence, the two states [8,4],[10,2] can be used to build momentum eigenstates:

$$\begin{aligned}|n,k_y=0\rangle &= [8,4] + e^{i\frac{2\pi n}{N}}[14,10] = [8,4] + e^{i\frac{2\pi n}{N}}[2,10]\\ &= [8,4] - e^{i\pi n}[10,2],\end{aligned} \tag{49}$$

where we have used $N = 2$ and $[2,10] = -[10,2]$ because the particles are fermions. The action of the relative translation operator gives

$$\begin{aligned}\tilde{T}_i(pL_x\hat{x})|0,k_y\rangle &= [14,10] - [16,8] = [2,10] - [4,8]\\ &= |0,k_y\rangle,\end{aligned} \tag{50}$$

and hence this state has momentum $k_x = 0$. Similarly, the state $|1,k_y\rangle$ has momentum $k_x = 2\pi/L_x$. Of the original three states at momentum $k_y = 0$, we now have to analyze [9,3].

TABLE I. Admissible (1,3) configurations (not more than one particle in three consecutive orbitals) for $N_e = 2$ particles in $N_\phi = 12$ orbitals. The total number of such configurations (42) equals the number of zero modes of the Haldane pseudopotential Hamiltonian whose highest density ground state is the Laughlin state. We have $N = 2$ and hence two k_y possible momenta, $0,\pi/L_y$.

No.\λ	0	1	2	3	4	5	6	7	8	9	10	11	$[\lambda_1,\lambda_2]$	$\sum\lambda_i$	$\sum\lambda_i$ mod N_ϕ	$\sum\lambda_i$ mod N
1	1	0	0	1	0	0	0	0	0	0	0	0	[3,0]	3	3	1
2	1	0	0	0	1	0	0	0	0	0	0	0	[4,0]	4	4	0
3	1	0	0	0	0	1	0	0	0	0	0	0	[5,0]	5	5	1
4	1	0	0	0	0	0	1	0	0	0	0	0	[6,0]	6	6	0
5	1	0	0	0	0	0	0	1	0	0	0	0	[7,0]	7	7	1
6	1	0	0	0	0	0	0	0	1	0	0	0	[8,0]	8	8	0
7	1	0	0	0	0	0	0	0	0	1	0	0	[9,0]	9	9	1
8	0	1	0	0	1	0	0	0	0	0	0	0	[4,1]	5	5	1
9	0	0	1	0	0	1	0	0	0	0	0	0	[5,2]	7	7	1
10	0	0	0	1	0	0	1	0	0	0	0	0	[6,3]	9	9	1
11	0	0	0	0	1	0	0	1	0	0	0	0	[7,4]	11	11	1
12	0	0	0	0	0	1	0	0	1	0	0	0	[8,5]	13	1	1
13	0	0	0	0	0	0	1	0	0	1	0	0	[9,6]	15	3	1
14	0	0	0	0	0	0	0	1	0	0	1	0	[10,7]	17	5	1
15	0	0	0	0	0	0	0	0	1	0	0	1	[11,8]	19	7	1
16	0	1	0	0	0	1	0	0	0	0	0	0	[5,1]	6	6	0
17	0	0	1	0	0	0	1	0	0	0	0	0	[6,2]	8	8	0
18	0	0	0	1	0	0	0	1	0	0	0	0	[7,3]	10	10	0
19	0	0	0	0	1	0	0	0	1	0	0	0	[8,4]	12	0	0
20	0	0	0	0	0	1	0	0	0	1	0	0	[9,5]	14	2	0
21	0	0	0	0	0	0	1	0	0	0	1	0	[10,6]	16	4	0
22	0	0	0	0	0	0	0	1	0	0	0	1	[11,7]	18	6	0
23	0	1	0	0	0	0	1	0	0	0	0	0	[6,1]	7	7	1
24	0	0	1	0	0	0	0	1	0	0	0	0	[7,2]	9	9	1
25	0	0	0	1	0	0	0	0	1	0	0	0	[8,3]	11	11	1
26	0	0	0	0	1	0	0	0	0	1	0	0	[9,4]	13	1	1
27	0	0	0	0	0	1	0	0	0	0	1	0	[10,5]	15	3	1
28	0	0	0	0	0	0	1	0	0	0	0	1	[11,6]	17	5	1
29	0	1	0	0	0	0	0	1	0	0	0	0	[7,1]	8	8	0
30	0	0	1	0	0	0	0	0	1	0	0	0	[8,2]	10	10	0
31	0	0	0	1	0	0	0	0	0	1	0	0	[9,3]	12	0	0
32	0	0	0	0	1	0	0	0	0	0	1	0	[10,4]	14	2	0
33	0	0	0	0	0	1	0	0	0	0	0	1	[11,5]	16	4	0
34	0	1	0	0	0	0	0	0	1	0	0	0	[8,1]	9	9	1
35	0	0	1	0	0	0	0	0	0	1	0	0	[9,2]	11	11	1
36	0	0	0	1	0	0	0	0	0	0	1	0	[10,3]	13	1	1
37	0	0	0	0	1	0	0	0	0	0	0	1	[11,4]	15	3	1
38	0	1	0	0	0	0	0	0	0	1	0	0	[9,1]	10	10	0
39	0	0	1	0	0	0	0	0	0	0	1	0	[10,2]	12	0	0
40	0	0	0	1	0	0	0	0	0	0	0	1	[11,3]	14	2	0
41	0	1	0	0	0	0	0	0	0	0	1	0	[10,1]	11	11	1
42	0	0	1	0	0	0	0	0	0	0	0	1	[11,2]	13	1	1

As it is a single state, it forms an orbit by itself. This is indeed true, as $[9+6,3+6] = [15,9] \equiv [3,9] = -[9,3]$. Due to the fermionic sign, this is state at momentum $k_x = 2\pi/L_x$. We have now determined that we have 1 zero mode state at momentum $k_x,k_y = 0,0$ and 2 at momentum $k_x,k_y = 2\pi/L_x,2\pi/L_y$. Note that, of course, our choice of which states to pick for the $k_y = 0$ momentum is irrelevant, giving the same counting. If instead we had picked the set of $k_y = 0$ states [9,5],[10,4],[11,3], then $[9,5] - [11,3]$ would be the state at $k_x = 0$, while $[9,5] + [11,3]$ and [10,4] would be the state at momentum $k_x = 2\pi/L_x$. This completes the symmetry analysis of the zero modes of 2 particles in $N_\phi = 12$ of the Haldane pseudopotential Hamiltonian for the Laughlin state at $k_y = 0$.

We now look at $k_y = 2\pi/L$ sector with the states denoted by the partitions [8,5],[9,4],[10,3],[11,2]. The orbit of [8,5] is $[2,11] \equiv -[11,2]$, while the orbit of [9,4] is $[3,10] \equiv -[10,3]$. Hence, the state $[8,5] - [11,2]$ has momentum $k_x = 0$, while $[8,5] + [11,2]$ has $k_x = 2\pi/L_x$. Identically, $[9,4] - [10,3]$ and $[9,4] + [10,3]$ have momenta $k_x = 0,\pi/L_x$. Hence, there are two states for $k_x = 0$ and two states for $k_x = 2\pi/L_x$. The same counting would be obtained if we picked any of the other states at $k_y = 2\pi/L_y$. We have now given a combinatoric prescription for counting the states per momentum sector

TABLE II. Partitions $[\lambda_1,\lambda_2]$ sorted by identical $\sum_i \lambda_i \bmod N_\phi$.

$\sum \lambda_i \bmod N_\phi$	$[\lambda_1,\lambda_2]$	$\sum \lambda_i \bmod N$
0	[8,4]; [9,3]; [10,2]	0
1	[8,5]; [9,4]; [10,3]; [11,2]	1
2	[9,5]; [10,4]; [11,3]	0
3	[3,0]; [9,6]; [10,5]; [11,4]	1
4	[4,0]; [10,6]; [11,5]	0
5	[5,0]; [4,1]; [10,7]; [11,6]	1
6	[6,0]; [5,1]; [11,7]	0
7	[7,0]; [5,2]; [11,8]; [6,1]	1
8	[8,0]; [6,2]; [7,1]	0
9	[6,3]; [7,2]; [8,1]; [9,0]	1
10	[7,3]; [8,2]; [9,1]	0
11	[7,4]; [8,3]; [9,2]; [10,1]	1

of the relative translation operators. For two particles in 12 orbitals the quasiholes of the Laughlin state have the following quantum numbers: 2 states in each of the k_x,k_y equal to $0,2\pi/L_y$, $2\pi/L_x,0$, and $2\pi/L_x,2\pi/L_y$ momenta, and 1 state in the 0,0 momentum. There is sixfold center of mass degeneracy which multiplies these 7 states to obtain the total of 42 quasihole states.

As a last simple example, let us look at resolving the quantum numbers of the bosonic ground states of the Haldane pseudopotential for the MR interaction for $N_e = 4$ particles in $N_\phi = 4$ fluxes. As $N_e/N_\phi = 1$ there is no center-of-mass degeneracy and the BZ of the relative translation operators is a 4×4 momenta. We first write down all the $(k,r) = (2,2)$ partitions (whose counting corresponds to the bosonic MR state) of four particles in four orbitals. They are, in occupation number 2020, 0202, 1111, totaling three, the correct non-Abelian degeneracy of the MR state, and they correspond to the partitions $\lambda = [2,2,0,0],[3,3,1,1],[3,2,1,0]$, respectively. We first sort the states by $\sum_{i=1}^4 \lambda_i (\mathrm{mod}\, 4)$, which gives 0,0,2. The $\sum_{i=1}^4 \lambda_i (\mathrm{mod}\, 4) = 2$ state is [3,2,1,0] and has $e^{-ik_y L_y/4} = e^{i2\pi\cdot 2/4}\cdot(-1)$, the $-$ sign coming from $pq(N_e-1)$ being odd. Hence, $k_y = 0$. We now find its k_x: $\tilde{T}_i(pL_x\hat{x})[3,2,1,0] = [4,3,2,1] \equiv [0,3,2,1] \equiv [3,2,1,0]$ by virtue of the bosonic nature of the state. Hence, $e^{-ik_x L_x/N} = -1$ or $k_x = 4\pi/L_x$. There is one state at $k_x,k_y = 4\pi/L_x,0$. The two other states [2,2,0,0],[3,3,1,1] belong to the $k_y = 4\pi/L_y$ sector and to the same orbit. We hence form the states

$$
\begin{aligned}
|0,k_y\rangle &= [2,2,0,0] + [3,3,1,1],\\
|1,k_y\rangle &= [2,2,0,0] + e^{i\frac{\pi}{2}}[3,3,1,1] = [2,2,0,0] + i[3,3,1,1],\\
|2,k_y\rangle &= [2,2,0,0] - [3,3,1,1],\\
|3,k_y\rangle &= [2,2,0,0] + e^{i\frac{3\pi}{2}}[3,3,1,1] = [2,2,0,0] - i[3,3,1,1].
\end{aligned}
\tag{51}
$$

It is clear that two states [2,2,0,0], [3,3,1,1] cannot be made into the four independent momentum states above. Indeed, this is because $|1,k_y\rangle,|3,k_y\rangle$ are not momentum eigenstates; for example, $\tilde{T}_i(pL_x\hat{x})|1,k_y\rangle = i|3,k_y\rangle$. The only two momentum eigenstates are $|0,k_y\rangle$ at momentum $k_x = 4\pi/L_x$ and $|2,k_y\rangle$ at momentum $k_x = 2\pi(4 \bmod N)/L_x = 0$. We now found that our combinatoric counting principle predicts that the zero modes of the Haldane pseudopotential for which the MR wave function is the ground state are resolved by the relative translation operators into momenta k_x,k_y equal to $(4\pi/L_x,0)$, $(0,4\pi/L_y)$, and $4\pi/l_x,4\pi/L_y)$. An exact diagonalization of the Hamiltonian confirms this.

It is immediately obvious that the current example can be easily generalized to all the (k,r) states. Our procedure allows for a combinatoric approach to resolving the number of quasiholes per momentum sector just by counting partitions. It goes beyond the usual counting on the one-dimensional-torus momentum which can only give the total number of quasiholes per one-dimensional momentum. More examples and data for Abelian and non-Abelian states are presented in the section which uncovers the mapping of FQH to FCI.

IV. EMERGENT MANY-BODY SYMMETRIES IN THE FRACTIONAL CHERN INSULATOR

In this section we show the appearance of many-body translational symmetry operators in the FCI. We first rederive the result, obtained in Ref. 15 and rederived in Ref. 33, that the long-wavelength algebra of the projected density operators in a Chern insulator has a GMP form when the Berry curvature variation is not large. We show that the noncommutativity of the projected density matrices is required by the nonzero Chern number in the nontrivial Chern insulator. We then show that the problem of a Hamiltonian with such a projected density algebra can be mapped into a FQH problem of a translationally invariant Hamiltonian *superimposed* on a background lattice of $N_x \times N_y (= N_\phi)$ sites. We then show that this problem admits relative translational operators and momenta which are a folding of the ones obtained in the FQH case in the continuum.

A. One-body projected density algebra of an insulator

In this section, we rederive the result obtained in Ref. 15. We work with translationally invariant one-body Hamiltonians,

$$H = \sum_{i,j,\alpha,\beta} c^\dagger_{i\alpha} h_{i-j;\alpha,\beta} c_{j\beta}, \tag{52}$$

where α,β contain orbital and spin indices. We call α an orbital index. We now quickly introduce some conventions. Our Fourier transform sign convention is $c_{k\alpha} = \frac{1}{\sqrt{N_s}} \sum_j e^{-ikj} c_{j\alpha}$, where by kj we mean $\vec{k}\cdot\vec{j}$ and N_s is the number of sites on a lattice with aspect ratio $N_x \times N_y$. The Bloch Hamiltonian matrix is $h_{\alpha\beta}(k) = \frac{1}{\sqrt{N_s}} \sum_r e^{-ikr} h_{r;\alpha,\beta}$. The Bloch Hamiltonian can be separated into normal mode operators γ^n_k at momentum k of the band n $H = \sum_{k,n} E_n(k) \gamma^{n\dagger}_k \gamma^n_k$, where the normal modes can be written as a matrix rotation of the original electron operators $\gamma^n_k = \sum_\beta u^{n\star}_{k,\beta} c_{k,\beta}$. The elements of the matrix are $u^{n\star}_{k,\beta}$, which form the eigenstates of the Bloch Hamiltonian $\sum_\beta h_{\alpha\beta}(k) u^n_{k,\beta} = E_n(k) u^n_{k,\alpha}$. We then define the projector into the band n at momentum k by

$$P_{nk} = \gamma^{n\dagger}_k |0\rangle\langle 0| \gamma^n_k. \tag{53}$$

Fractional topological insulators are usually constructed and observed in models with fractionally filled bands whose bandwidth is very small, such that interactions and not the kinetic energy dominate the physics. The ideal example of

such an insulator is the flat band one-body deformation of any Hamiltonian insulator $h(k)$:

$$H_{FB} = -\sum_{n_1, E_{n_1,k}<\mu} P_{n_1,k} + \sum_{n_2, E_{n_2,k}>\mu} P_{n_2,k}. \quad (54)$$

From now on, we consider the physics of the (fractionally) occupied bands and look only at projectors into the occupied bands. We define the density operator per orbital α at site j, $\rho_j^\alpha = c_{j\alpha}^\dagger c_{j\alpha}$, whose Fourier transform reads $\rho_q^\alpha = \frac{1}{\sqrt{N_s}}\sum_j e^{-iqj}\rho_j^\alpha = \frac{1}{\sqrt{N_s}}\sum_k c_{\alpha,k}^\dagger c_{\alpha,k+q}$. Notice that we do not shift the sum to put $k+q/2, k-q/2$ because, while perfectly suitable in the continuum, that would change the boundary conditions on a lattice at which q_i is quantized in units of $2\pi/N_i$ $(i = x, y)$.

As we are interested in the low-energy physics in the fractionally filled bands, we define the projected density operator $\tilde{\rho}_{k_1,q,k_2}^{n_1,\alpha,n_2} = P_{n_1,k_1}\rho_q^\alpha P_{n_2,k_2}$, which has the following form: $\tilde{\rho}_{k_1,q,k_2}^{n_1,\alpha,n_2} = \frac{1}{\sqrt{N_s}} u_{\alpha,k_1}^{n_1\star} u_{\alpha,k_1+q}^{n_2}\delta_{k_2,k_1+q}\gamma_{k_1}^{n_1\dagger}|0\rangle\langle 0|\gamma_{k_1+q}^{n_2}$ The full projected density involves a summation over the orbital α, and over the projection operators $P = \sum_{k,n} P_{n,k}$:

$$\tilde{\rho}_q = \frac{1}{\sqrt{N_s}}\sum_{n_1,n_2,\alpha,k} u_{\alpha,k}^{n_1\star} u_{\alpha,k+q}^{n_2}\gamma_k^{n_1\dagger}|0\rangle\langle 0|\gamma_{k+q}^{n_2}. \quad (55)$$

Taking two densities at momenta q and w, we obtain

$$[\rho_q,\rho_w] = \frac{1}{N_s}\sum_{k,n_1,n_2,m_2,\alpha,\beta}\left(u_{\alpha,k_1}^{n_1\star}u_{\alpha,k+q}^{n_2}u_{\beta,k+q}^{n_2\star}u_{\beta,k+w+q}^{m_2} - u_{\beta,k}^{n_1\star}u_{\beta,k+w}^{n_2}u_{\alpha,k+w}^{n_2\star}u_{\alpha,k+w+q}^{m_2}\right)\gamma_k^{n_1\dagger}|0\rangle\langle 0|\gamma_{k+q+w}^{m_2}. \quad (56)$$

We particularize to the low-wavelength continuum limit $q \ll 1$ (in lattice constant units). On a discrete lattice, low q represents a small integer combination of $2\pi/N_i$. In this limit, a Taylor expansion gives

$$u_{\alpha,k+q}^n = u_{\alpha,k}^n + q_i\partial_i u_{\alpha,k}^n + \tfrac{1}{2}q_iq_j\partial_i\partial_j u_{\alpha,k}^n, \quad (57)$$

where ∂'s denote discrete momentum derivatives. We expand the difference in Eq. (56) in the wavelength limit and use the identities $\sum_\alpha u_{\alpha,k_1}^{n_1\star}u_{\alpha,k_1}^{n_2} = \delta_{n_1,n_2}$, $\sum_\alpha(\partial_i u_{\alpha,k_1}^{n_1\star})u_{\alpha,k_1}^{n_2} + u_{\alpha,k_1}^{n_1\star}\partial_i u_{\alpha,k_1}^{n_2} = 0$ and

$$A_{ij}\left[2\left(\partial_i u_{\alpha,k_1}^{n_1\star}\right)\left(\partial_j u_{\alpha,k_1}^{n_2}\right) + \left(\partial_i\partial_j u_{\alpha,k_1}^{n_1\star}\right)u_{\alpha,k_1}^{n_2} + u_{\alpha,k_1}^{n_1\star}\left(\partial_j\partial_j u_{\alpha,k_1}^{n_2}\right)\right] = 0 \quad (58)$$

(valid for A_{ij} a symmetric tensor) to find, after tedious algebra (presented in Appendix A), that in the long-wavelength limit,

$$\sum_{n_2} u_{\alpha,k}^{n_1\star}u_{\alpha,k+q}^{n_2}u_{\beta,k+q}^{n_2\star}u_{\beta,k+w+q}^{m_2} - u_{\beta,k}^{n_1\star}u_{\beta,k+w}^{n_2}u_{\alpha,k+w}^{n_2\star}u_{\alpha,k+w+q}^{m_2} \approx \frac{i}{2}(q_iw_j - w_iq_j)F_{ij}^{n_1m_2}, \quad (59)$$

where $F_{ij}^{n_1,m_2}$ is the non-Abelian field strength, $F_{ij}^{n_1,m_2} = \partial_i A_j^{n_1,m_2} - \partial_j A_i^{n_1,m_2} - i[A_i,A_j]^{n_1,m_2}$, with the Berry potential $A_j^{n_1n_2} = -i\sum_\beta u_\beta^{n_1\star}\partial_j u_\beta^{m_2}$ the non-Abelian field strength. Reference 15 hence finds

$$[\rho_q,\rho_w] = -\frac{i}{2}(q_iw_j - w_iq_j)\frac{1}{N_s} \times \sum_{k,n_1,m_2} F_{ij}^{n_1,m_2}\gamma_k^{n_1\dagger}|0\rangle\langle 0|\gamma_{k+q+w}^{m_2}. \quad (60)$$

The difference with the result of Ref. 15 is only apparent because we are working in the low-wavelength limit q, w small and we kept terms to second order in q, w, to the order in perturbation theory that we are working at; we have that $\sum_b u_b^{\alpha\star}(k_+)u_b^\alpha(k_-) \approx \sum_b u_b^{\alpha\star}(k_+)u_b^\alpha(k) = 1$, which proves the equivalence between the formula in Ref. 15 and the above. The smallest q_x, w_y are $q_x = 2\pi/N_x$ and $q_y = 2\pi/w_y$.

Before we investigate the full implications of this result, we point out three important results. First, the commutator of two densities has to be nonzero in a nontrivial Chern insulator. That is so because the Chern number of the insulator can be expressed as a trace over the density commutator, as shown in Appendix B. Second, the commutator of densities at the smallest available lattice momentum $2\pi/(N_xa), 2\pi/(N_ya)$ with a the lattice constant is identical to the commutator of the projected X and Y lattice position operators, as shown in Appendix C. The trace of this commutator is known to give the Chern number. Third, as a bonus, the expression of the Chern number in terms of the commutator of the projected X, Y coordinates allows for a direct derivation of the Chern number of the continuum Landau level, which was not possible with the usual Thouless, Kohmoto, Nightingale, and den Nijs formula for the Chern number which involve derivatives over the two momenta. We show this in Appendix D.

B. Girvin-MacDonald-Platzman algebra for insulators with smooth Berry curvature

We now particularize to two-band models (insulators with one band below and above the gap) or to many-band insulators where the non-Abelian components of the field strength can be neglected. We observe that the commutator in Eq. (60) does not form an algebra as the right-hand side is not easily expressible in terms of a density operator. However, the commutator algebra has an eerie similarity to a GMP algebra at long wavelength. As pointed out in Ref. 15, if the local Berry curvature can be replaced by its average,

$$F_{ij}(k) = \epsilon_{ijm}B_m(k) = \epsilon_{ij}\frac{\int_{BZ} d^2k B_m(k)}{\int_{BZ} d^2k} = \frac{2\pi C}{(2\pi/a)^2}\hat{z}, \quad (61)$$

where C is the band Chern number. We then observe that the field strength can be taken out of the sum in Eq. (60), and, to zeroth order in $q+w$, $\rho_{q+w} = \sum_k \gamma_k^{n\dagger}|0\rangle\langle 0|\gamma_{k+q+w}^m + O(q+w)$. The commutator algebra then becomes

$$[\rho_q,\rho_w] = -i(\vec{q}\times\vec{w})\cdot\hat{z}\frac{2\pi C}{(2\pi/a)^2}\rho_{q+w}, \quad (62)$$

which is identical to the GMP algebra at small q. Several comments are now necessary. First, in a two-band insulator, it is impossible to have a constant Berry curvature due to the no-hair theorem,[34] although this seems possible in insulators with four or more bands.[34] However, we from now on assume that this is indeed possible, and assume the validity, at low energies of the GMP algebra for Chern insulators. We then

observe that the density algebra for the Chern insulator is identical for low momenta to the one for the Landau level QH problem if

$$(\vec{q}\times\vec{w})\cdot\hat{z}\frac{2\pi}{(2\pi/a)^2}=(\vec{q}_1\times\vec{q}_2)\cdot\hat{z}l^2, \tag{63}$$

where q,w are the smallest values of the momentum on the lattice: $\vec{q}=2\pi/(N_x a)\hat{x}$, $\vec{w}=2\pi/(N_y a)\hat{y}$ while $\vec{q}_1=2\pi\vec{L}_2/\mathcal{A}$, $\vec{q}_2=-2\pi\vec{L}_1/\mathcal{A}$ are the smallest momenta of the QH torus. $\mathcal{A}=(\vec{L}_1\times\vec{L}_2)\cdot\hat{z}=2\pi l^2 N_\phi$ is the area of the continuum torus BZ, $(2\pi/a)^2$ is the area of the BZ on the lattice, and we specialized, without loss of generality to a square lattice. Since the lowest Landau level (LLL) has Chern number 1 (see Appendix D), we also took $C=1$. We hence have $(\vec{q}_1\times\vec{q}_2)\cdot\hat{z}l^2=(2\pi)^2l^2/\mathcal{A}=2\pi/N_\phi=(\vec{q}\times\vec{w})\cdot\hat{z}\frac{2\pi C}{(2\pi/a)^2}=2\pi/(N_xN_y)$, which leads us to the equivalence of the GMP algebras for a Chern insulator with Chern number 1 on a lattice with N_x,N_y sites in the x,y directions and the algebra of the QH effect on a torus pierced by N_ϕ flux quanta *if*

$$N_\phi=N_x\cdot N_y. \tag{64}$$

An important remark should be made here. As pointed out in Ref. 15, it is important to realize that there is no one-to-one mapping between the Chern insulator density algebra and the FQH one. First, the FCI density GMP algebra is valid only at long wavelengths, and it will be our *assumption* that as system sizes reach thermodynamic limit, its application transcends the long-wavelength limit and it becomes an approximate symmetry of the system at *all* wavelengths. This is indeed justified *a posteriori* by our extensive numerical checks, which prove the existence of center-of-mass degeneracies in the Chern insulator which would be possible only if the many-body translational operators obeyed GMP algebra for *all* wavelengths. Second, the number of density generators in the FCI and FQH differ (N_s in the FCI, N_s^2 in the FQH),[15] but, as was pointed out in Ref. 15, there are many instances when the significant physics is governed only by the N_s operators in the FCI.

C. Fractional quantum Hall to fractional Chern insulator mapping

We now found that the constant Berry curvature Chern insulator density algebra is identical to that of electrons in a uniform magnetic field with number of fluxes $N_\phi=N_x\cdot N_y$. Hence, the translational symmetries of the two problems should share similarities. To complete the analogy, since the Chern insulator is defined on a lattice, we need to introduce a lattice to the FQH problem. We are then led to consider the translational symmetries of the Hamiltonian in magnetic field:

$$H=\frac{1}{2m}\sum_j^{N_e}\Pi_j^2+\frac{1}{2\mathcal{A}}\sum_{\vec{q}}V(\vec{q})\sum_{i<j}e^{i\vec{q}\cdot(\vec{r}_i-\vec{r}_j)}$$
$$+V_0\sum_{i=1}^{N_e}\sum_{m=1}^{N_x}\sum_{n=1}^{N_y}\delta(\vec{r}_i-ml_x\hat{x}-nl_y\hat{y}), \tag{65}$$

with $\Pi_j=-i\hbar\nabla_j-eA(r_j)=-i\hbar\nabla_j+|e|A(r_j)$ the canonical momentum in the presence of a magnetic field. N_e is the number of electrons in the system. We choose not to gauge fix and have $\vec{\nabla}\times\vec{A}=\vec{B}$. The positions of the particles, $\{\vec{r}_i\}$, reside on a two-dimensional torus of generators $\vec{L}_1$, $\vec{L}_2$. The Hamiltonian is periodic under translations by these vectors, $V(\vec{r}_i-\vec{r}_j)=(\vec{r}_i-\vec{r}_j+\vec{L}_{1,2})$ and can be written as a sum over the allowed reciprocal vectors $\vec{q}$. $\mathcal{A}=|\vec{L}_1\times\vec{L}_2|$ is the area of the sample, and $\vec{q}=m\vec{q}_1+n\vec{q}_2$, $m,n\in\mathbb{Z}$ and $\vec{q}_1=\frac{2\pi}{\mathcal{A}}\vec{L}_2\times\hat{z}$, $\vec{q}_2=-\frac{2\pi}{\mathcal{A}}\hat{z}\times\vec{L}_1$. We choose to work on a square lattice, without any loss of generality. If the Hamiltonian of Eq. (65) was made out of only the first two terms, the symmetry analysis would have been identical to the one presented in Sec. III and the number of states of any model FQH state per momentum sector would have been obtainable by our constructive procedure of implementing the relative translational symmetries in both x,y directions on the (k,r)-generalized Pauli principle states.

The last term of Eq. (65) implements the lattice with N_x sites in the x direction and N_y sites in the y. The lattice constants in the x,y directions are $l_x=L_1/N_x$, $l_y=L_2/N_y$. It makes electrons energetically favorable (for large negative V_0) to sit on lattice sites, and it makes the momenta in the x,y direction take the discretized set of values $(\vec{q}\cdot\hat{x},\vec{q}\cdot\hat{y})=(2\pi i/(N_xl_x),2\pi j/(N_yl_y))$, with $i=0,\ldots,N_x$, $j=0,\ldots,N_y$, which also serve as the momenta of the many-body states. The problem defined by Eq. (65) is similar to that of the Chern insulator: It has the same density algebra in the long-wavelength limit, the same lattice, and the same translationally invariant Hamiltonian. The two-body Hamiltonian can be replaced by an n-body Hamiltonian, as long as it is translationally invariant. A physical assumption is then the fact that the low-energy spectrum of the FQH and FCI problems (when the FCI problem has a topologically ordered ground state) will be similar. More to the point, we take it as a proof of the topological nature of the FCI state that the low-energy manifold of states has the identical counting, per momentum sector, to that of the FQH states at the same filling *in the presence of the lattice* in Eq. (65). We now find what that counting is.

The presence of the lattice influences the symmetries of the problem. The set of continuum translation operators $T_i(\vec{a})$ is not valid unless $\vec{a}$ is a multiple of the lattice constants $l_x\hat{x},l_y\hat{y}$. Hence, translational symmetry operators are $T_i(m_xl_x\hat{x}),T_i(m_yl_y\hat{y})$. Although the one-body terms of Eq. (65) commute with $T_i(l_x\hat{x}),T_i(l_y\hat{y})$, due to the many-body interacting term (which does not commute with those operators), the Hamiltonian still commutes only with $T_i(N_xl_x\hat{x}),T_i(N_yl_y\hat{y})$. The Hilbert space is described by the two twist parameters:

$$T_i(N_xl_x\hat{x})|\psi\rangle=e^{i\theta_x}|\psi\rangle,\quad T_i(N_yl_y\hat{y})|\psi\rangle=e^{i\theta_y}|\psi\rangle. \tag{66}$$

As the number of fluxes per unit cell plaquette is $N_\phi/(N_xN_y)=1$, the translational operators of unit cell length commute: $[T_i(l_x\hat{x}),T_j(l_y\hat{y})]=-2\delta_{ij}T_i(l_x\hat{x}+l_y\hat{y})\sin(l_xl_y/2l^2)=0$, since $l_xl_y/2l^2=L_xL_y/2l^2N_xN_y=2\pi l^2N_\phi/2l^2N_xN_y=\pi$. The center-of-mass translation operator $T(\vec{a})=\prod_{i=1}^{N_e}T_i(\vec{a})$ commutes with the translation operator $T_i(l_x\hat{x})$ or $T_i(l_y\hat{y})$ if $\vec{a}=l_x\hat{x}$ or $l_y\hat{y}$. Notice that the operator $T(\vec{L}_1/N_\phi)$ [or

$T(\vec{L}_2/N_\phi)$], which commuted with $T_i(\vec{L}_2)$, [or $T_i(\vec{L}_1)$, respectively] in the continuum limit, does not appear here because $L_1/N_\phi = L_1/(N_xN_y) = l_x/N_y$ is smaller than the permissible lattice constant. Hence, the center of mass translation operators commute between themselves and the *exact* q-fold degeneracy apparent in the continuum FQH is reduced to a onefold degeneracy of any sector (in other words, we do not have exact degeneracies anymore). However, *if* by adding the lattice we still remain in the FQH state, then remnants of the original degeneracies and spectrum in the continuum should appear even after adding the lattice. In particular, we know the counting of the degenerate zero-mode quasihole states (for FQH series such as RR) in the continuum, where they are zero modes of pseudopotential Hamiltonians. We now try to find what the counting is on the lattice momentum.

As we know the counting of the FQH per continuum momentum of the relative translational operators, we now try to implement the relative translational symmetries of the problem. The relative translation operators in the continuum, $\tilde{T}_i(\vec{a}) = T_i[(N_e-1)\vec{a}/N_e]\prod_{j\neq i}^{N_e} T_i(-\vec{a}/N_e)$, make sense only if a/N_e is a multiple of l_x or l_y, and hence the relative translation operators by the smallest amount are

$$\tilde{T}_i(N_e l_x\hat{x}) = T_i[(N_e-1)l_x\hat{x}]\prod_{j\neq i} T_j(-l_x\hat{x}), \tag{67}$$

and similarly for l_y. We now ask two questions: Do these operators commute with $T_i(\vec{L}_1), T_i(\vec{L}_2)$ *and* do they commute with the Hamiltonian of the problem? The answer to the first question is an unequivocal yes, as $L_1 l_y/2l^2 = L_x L_y/2l^2 N_y = \pi N_\phi/N_y = \pi N_x$). The answer to the last question is *no*, because $\tilde{T}_i(N_e l_x\hat{x})$ commutes with $\exp[i\vec{q}\cdot(\vec{r}_j - \vec{r}_l)]$ when $j,l \neq i$, as it translates both coordinates by the same amount but does not commute with $\exp[i\vec{q}\cdot(\vec{r}_i - \vec{r}_l)]$,

$$\begin{aligned}&\tilde{T}_i(N_e l_x\hat{x})e^{i\vec{q}(\vec{r}_i-\vec{r}_l)}\\ &\quad= e^{i\vec{q}(\vec{r}_i+(N_e-1)l_x\hat{x})}e^{-i\vec{q}\cdot(\vec{r}_l-l_x\hat{x})}e^{i\vec{q}(\vec{r}_i-\vec{r}_l)}\tilde{T}_i(N_e l_x\hat{x})\\ &\quad= e^{i\vec{q}\cdot\hat{x}N_e l_x}e^{i\vec{q}(\vec{r}_i-\vec{r}_l)}\tilde{T}_i(N_e l_x\hat{x}),\end{aligned} \tag{68}$$

since $\vec{q}\cdot\hat{x} = 2\pi j/N_x l_x$, $j = 0,1,\ldots,N_x$, and hence $N_e l_x = 2\pi N_e/N_x$; an identical situation obviously occurs for $\tilde{T}_i(N_e l_y\hat{y})$. As N_e, N_x, N_y are integers, we now define several important ratios and common denominators:

$$\begin{aligned}&GCD(N_e,N_x) = N_{0x}, \quad GCD(N_e,N_y) = N_{0y},\\ &\frac{N_e}{N_x} = \frac{p_x}{q_x}, \quad \frac{N_e}{N_y} = \frac{p_y}{q_y}.\end{aligned} \tag{69}$$

The q_x, q_y are integers and should not be mistaken for the components of a q momentum vector. Fortunately, this mistake is hard to do from the context. There are obvious relations between the above and $N = GCD(N_e,N_\phi), N_e/N_\phi = p/q$, but we will come to this later. It is then clear to see which relative translation operators commute with the Hamiltonian:

$$\begin{aligned}&\tilde{T}_i(q_x N_e l_x\hat{x}) = T_i(q_x(N_e-1)l_x\hat{x})\prod_{j\neq i} T_j(-q_x l_x\hat{x}),\\ &\tilde{T}_i(q_y N_e l_y\hat{y}) = T_i(q_y(N_e-1)l_y\hat{y})\prod_{j\neq i} T_j(-q_y l_y\hat{y}).\end{aligned} \tag{70}$$

These operators commute with both translations and the Hamiltonian. They also commute between themselves and hence can be diagonalized (remember that in the Chern insulator, the commutations are only approximate, low-energy properties, as the GMP algebra is valid only at long wavelength). We now ask how many eigenvalues of these operators are independent. We use the same reasoning as in the continuum limit and assume that the many-body state experiences, when acted upon by $\sum_{i=1}^{N_e}\exp(i\vec{Q}\cdot\vec{r}_i)$, an increase in its momentum by $\vec{Q}$ as long as $\vec{Q}$ is an allowed lattice momentum $\exp(iQ_xL_1) = \exp(Q_yL_2) = 1$. The eigenvalues λ_k

$$\tilde{T}_i(q_x N_e l_x\hat{x} + q_y N_e l_y\hat{y})|\psi(k)\rangle = \lambda(k)|\psi(k)\rangle \tag{71}$$

can be easily obtained by following the continuum proof closely and satisfy $\lambda(k) = D\exp[-i(k_y q_y l_y - k_x q_x l_x)]$. The coefficient D can be determined by requiring that the $k=0$ state has maximum lattice symmetry, and hence $D|\psi(k=0)\rangle = \tilde{T}_i(q_y N_e l_y\hat{y})|\psi(k=0)\rangle = \tilde{T}_i(-q_x N_e l_x\hat{x})|\psi(k=0)\rangle = \tilde{T}_i(q_y N_e l_y\hat{y} - q_x N_e l_x\hat{x})|\psi(k=0)\rangle$. From here we obtain that $D = (-1)^{q_x q_y N_e(N_e-1)} = 1$ (notice the difference from the continuum case, in which D could be both $1,-1$). To obtain the values of different relative momenta, we notice that

$$[\tilde{T}_i(q_x N_e l_x\hat{x})]^{N_{0x}} = [\tilde{T}_i(q_y N_e l_y\hat{y})]^{N_{0y}} = 1, \tag{72}$$

which implies $\exp(-ik_x q_x N_{0x} l_x) = \exp(-ik_y q_y N_{0y} l_y) = 1$. Expectedly, $k_x = 2\pi j/N_x l_x$ and $k_y = 2\pi j/N_y l_y$ with $j = 1,2'\ldots$. Now that we obtained the values of the different momenta, we can ask how many of these eigenvalues are distinct. The eigenvalues appear as $\exp(ik_x q_x l_x) = \exp(i2\pi j q_x/N_x) = \exp(i2\pi j/N_{0x})$ and similarly for the y component, so the number of distinct momenta resolving the relative translation symmetry is

$$\begin{aligned}&k_x = \frac{2\pi j}{N_x l_x}, \quad j = 0,\ldots,N_{0x}-1;\\ &k_y = \frac{2\pi j}{N_y l_y}, \quad l = 0,\ldots,N_{0y}-1.\end{aligned} \tag{73}$$

This defines a $N_{0x}\times N_{0y}$ BZ. The momenta of the relative translational operators of the FCI, $k_x = \frac{2\pi j}{N_x l_x}$, $j = 0,\ldots,N_{0x}-1$; $k_y = \frac{2\pi j}{N_y l_y}$, $l = 0,\ldots,N_{0y}-1$, are in fact foldings of the $k_x = \frac{2\pi j}{L_x}$, $j = 0,\ldots,N$; $k_y = \frac{2\pi j}{L_y}$, $l = 0,\ldots,N$ momenta of the FQH. To show this, we first note that both N_{0x}, N_{0y} divide N. Indeed, since $GCD(N_x,N_e) = N_{0x}$, $GCD(N_y,N_e) = N_{0y}$, and $(N_s,N_e) = (N_xN_y,N_e) = N$, we have that $GCD(N_xN_y/N_{0x}, N_e/N_{0x}) = N/N_{0x} = GCD(q_xN_y, p_xN_{0x})$, which proves that N/N_{0x} is an integer and similarly for N/N_{0y}. With $N_e/N_s = p/q$, we have $N_e = pN = p_xN_{0x}$ and, hence, with $N = p_xN_{0x}/p = p_yN_{0y}/p$ we have that the FCI momentum quantum numbers k_x, k_y of the relative translation operator are a $p_x/p, p_y/p$ folding of the FQH momentum quantum numbers in the x,y directions, respectively. We have hence taken care of the relative momentum quantum numbers.

In the FQH in the continuum there is a center-of-mass degeneracy of q. This center-of-mass degeneracy comes from the noncommutativity of the continuum center-of-mass

translation operators $T_{\rm CM}(\vec{L}_{mn}/N_s)$. On the lattice, we also know that since

$$\tilde{T}_i(q_x N_e l_x \hat{x}) \cdot T_{\rm CM}(q_x l_x \hat{x}) = T_i(q_x N_e l_x \hat{x}), \qquad (74)$$

the eigenvalue of $T_{\rm CM}(q_x l_x \hat{x})$ is fixed once k_x and θ_x are known [similarly for $T_{\rm CM}(q_y l_y \hat{y})$]. Since we have already resolved the motion in the $N_{0x} \times N_{0y}$ BZ, we have a remainder of $q_x \times q_y$ momenta to reach the full lattice BZ of $N_x \times N_y$. $T_{\rm CM}(l_x \hat{x}), T_{\rm CM}(l_y \hat{y})$ form a maximally commuting set of center-of-mass operators which can be simultaneously diagonalized [note that in the FQH $T_{\rm CM}(\vec{L}_{mn}/N_s)$ could not be simultaneously diagonalized] and which commute with the Hamiltonian, so no exact degeneracies are generically present. However, if the system is in the same universality class as the FQH, the low-energy modes will then exhibit a center-of-mass q_x quasidegeneracy in the x direction and q_y quasidegeneracy in the k_y direction. This degeneracy, as well as the relative momentum, make up the full BZ of the $N_x \times N_y$ lattice. Note that in the lattice example, all translation operators commute with each other (courtesy of unit flux per unit cell), so, in effect, we could just diagonalize those. However, we choose to build the relative translational operators because in the continuum case we already know the counting per the momentum quantum number attached with these operators in the FQH. To obtain the counting of the eigenstates per FCI relative momentum, one needs to fold the FQH relative momentum BZ. This folding now needs to be supplemented by the mismatch in the center-of-mass degeneracy. In the FQH, the center-of-mass degeneracy is q; in the FCI, it is $q_x q_y$. In Appendix E we show that $q/(q_x q_y)$ is an integer number. The counting of states in the low-manifold, sorted, per FCI relative momentum sector is a folding of the FQH relative momentum BZ times the mismatch in center-of-mass degeneracy $q/(q_x q_y)$.

In conclusion, the diagonalization of a Chern insulator at fractional rational filling should exhibit, in the topologically ordered phase, a low-energy manifold of states with counting which encodes the topological character of the state. The low-energy manifold of states is a result of the emergent translational symmetry of the system that the long-wavelength GMP algebra implies. For a $N_x \times N_y$ lattice with N_e electrons, the states in this low manifold will experience an emergent center-of-mass degeneracy, with the spectrum being $q_x \times q_y$ quasidegenerate (in the k_x, k_y direction). If the state developing in the system is at filling p/q, the low-energy manifold will contain either the ground states or the quasihole excitations of this state. Once the center-of-mass degeneracy is resolved, the spectrum of the FCI per relative momentum sector is a folding of the spectrum of the FQH relative momentum BZ. We present clear examples of this procedure in the next section for the FCI at $1/3$ Abelian topological order before presenting numerical data on the Abelian and non-Abelian FCI states.

D. Two simple examples of the FQH to FCI mapping

We now look at two simple examples of how the analytical construction in the previous sections can be applied to the numerical data in both the energy and the entanglement spectra. The counting per momentum sector can be obtained from our FQH to FCI mapping. Lets first look at the specific

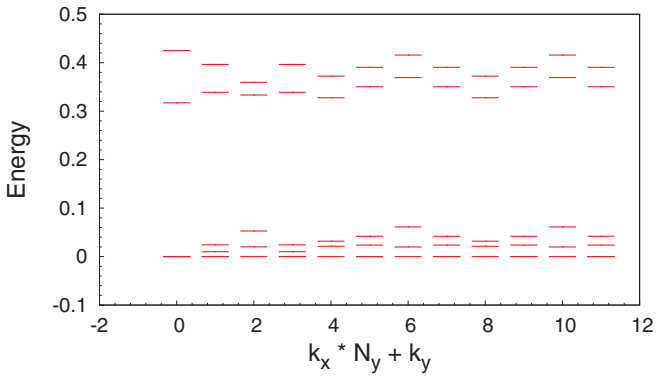

FIG. 2. (Color online) Energy spectrum for $N = 2, N_x = 3, N_y = 4$. The total number of states of the low-energy manifold the dotted line is 42. Per momentum sector, the counting is three states if k_y is divisible by two and four states otherwise, irrespective of k_x (there are degeneracies in the spectrum, for example, there are five states at momentum (0,0), the low-energy manifold being 3-fold degenerate with zero energy

case of such counting for $N_x \times N_y = 3 \times 4$ lattice Chern insulator model of Ref. 20 diagonalized in the flat-band limit[8] with $N_e = 2$ electrons and nearest-neighbor (on-site being forbidden) Hubbard interaction. This interaction favors a $1/3$ Abelian state, which we know occurs in the FQH state for short-range repulsive pseudopotentials. As the state contains only two particles, we expect that the physics is that of two-electron $\nu = 1/3$ Abelian FQH state plus a number of six quasiholes. The physics also reveals the structure of the pseudopotential two-body interaction in the FCI. The spectrum, shown in Fig. 2, confirms this. We observe a clear gap between a low-energy manifold of states and a high-energy manifold of spurious states. We focus on the low-energy manifold. By looking at the numerical data (Fig. 3, which includes degeneracies), we see that the low-energy manifold exhibits a counting of states of either three or four states per momentum sector, depending on whether k_y is divisible by 2, as can be seen in Fig. 3. This clearly shows that the spectrum is sixfold degenerate, and moreover, that this degeneracy splits in a k_x threefold degeneracy and a k_y twofold degeneracy. This is consistent with our analysis for $N_e/N_x = 2/3$, $N_e/N_y = 1/2$, which fix $q_x = 3, q_y = 2$. Since the $GCD(N_x, N_e) = 1$, while the $GCD(N_y, N_e) = 1$, the relative momentum BZ is made of $k_x = 0$ and $k_y = 0, 2\pi/(N_y a)$, where a is the lattice constant in the y direction. In this BZ, the counting of states is 3,4, respectively, while the whole counting in the full BZ of the FCI lattice is a 3×2 center-of-mass translation of this in the x, y directions, respectively (see Fig. 3). In the FQH effect, $N_e/N_s = 1/6$ and hence the center-of-mass degeneracy of $q = 6$ $(= q_x q_y)$ and there is no center-of-mass degeneracy mismatch between the FQH and the FCI. The FQH relative momentum BZ that remains after the center-of-mass degeneracy is removed is a 2×2 BZ $[GCD(N_s, N_e) = 2]$. The Laughlin $1/3$ Abelian FQH counting of quasihole states analysis was presented in Table I. In that section, we found that for two particles in 12 orbitals the quasiholes of the Laughlin state have the following quantum numbers: 2 states in each of the k_x, k_y equal to $0, 2\pi/L_y$, $2\pi/L_x, 0$, and $2\pi/L_x, 2\pi/L_y$ momenta, and 1 state in the 0,0 momentum. There is sixfold

kx	ky	Energy Spectrum
0	0	-1.3884765640985e-16
0	0	-4.9439619065339e-17
0	0	-1.5542732952087e-17
0	0	0.317240862227187
0	0	0.425121031580l4
0	1	-5.3341999697349e-17
0	1	5.0852621395482e-18
0	1	0.010048407799423
0	1	0.024274234312278
0	1	0.33888405091746
0	1	0.3963427291912
0	2	2.4978517862854e-17
0	2	0.020056085343729
0	2	0.052734525110249
0	2	0.333302175042l3
0	2	0.35954424708544
0	3	-7.1465790804661e-17
0	3	-2.5624513741419e-17
0	3	0.010048407799423
0	3	0.024274234312278
0	3	0.33888405091746
0	3	0.3963427291912
1	0	2.916745546161e-17
1	0	0.021249862859869
1	0	0.031708550030264
1	0	0.32757989004564
1	0	0.37230089303792
1	1	-3.898711728306 3e-17
1	1	4.4010679807738e-18
1	1	0.023620552543974
1	1	0.041962780470548
1	1	0.35043416487391
1	1	0.39043727630217
1	2	9.6026243394326e-18
1	2	0.019828470386375
1	2	0.061191955024663
1	2	0.3693832032406
1	2	0.41577794628172
1	3	-5.5357282492256e-17
1	3	2.2560202136414e-19
1	3	0.023620552543974
1	3	0.041962780470548
1	3	0.35043416487391
1	3	0.39043727630217
2	0	-8.445196894217 2e-20
2	0	0.021249862859869
2	0	0.031708550030264
2	0	0.32757989004564
2	0	0.37230089303792
2	1	-4.9198148211522e-17
2	1	-6.5298434542347e-18
2	1	0.023620552543974
2	1	0.041962780470548
2	1	0.35043416487391
2	1	0.39043727630216
2	2	-7.3500352028837e-18
2	2	0.019828470386375
2	2	0.061191955024663
2	2	0.3693832032406
2	2	0.41577794628172
2	3	-6.7468258047537e-18
2	3	3.0446807668924e-17
2	3	0.023620552543974
2	3	0.041962780470548
2	3	0.35043416487391
2	3	0.39043727630217

Low-Energy Manifold Counting for the FCI

(Momenta are in units of the smallest allowed lattice momentum)

kx Ny + ky	kx	ky	Counting
0	0	0	3
1	0	1	4
2	0	2	3
3	0	3	4
4	1	0	3
5	1	1	4
6	1	2	3
7	1	3	4
8	2	0	3
9	2	1	4
10	2	2	3
11	2	3	4

Relative momentum Brilloun zone counting

ky	Counting
0	3
1	4

Zero Mode Counting Per Relative Momentum Quantum Number of the FQH Haldane Pseudopotential for the 1/3 Abelian (Laughlin) FQH state

(Momenta are in units of the smallest allowed momentum)

kx	ky	Counting
0	0	1
0	1	2
1	0	2
1	1	2

Fold the FQH relative momentum BZ to get to the FCI

kx	ky	Counting
0	0	1+2=3
0	1	2+2=4

FIG. 3. (Color online) Example of the FQH to FCI mapping for $N_e = 2$, $N_x = 3$,$N_y = 4$ state. The spectrum of the one-body flat-band Chern Hamiltonian[20] with nearest-neighbor interaction is given on the left. The counting of the low-energy manifold of states exhibits clear center-of-mass degeneracies and the relative momentum BZ of the FCI is a 1×2 BZ. The counting per momentum sector in this BZ is a folding of the counting of zero modes of the Haldane FQH pseudopotential whose highest density state is the Laughlin state. This implies that the universality class of the FCI state is the same as that of the $\nu = 1/3$ state.

center-of-mass degeneracy which multiplies these 7 states to obtain the total of 42 quasihole states. Our theory then implies that the counting of the FCI per relative momentum sector is a $p_x/p = 2$ folding of the FQH relative momentum BZ. This folding gives a $2 + 1,2 + 2$ counting for the $k_x = 0$ and $k_y = 0,2\pi/(N_y a)$ momenta, respectively, which perfectly agrees with the numerical data (see Fig. 3).

For larger number of particles and quasiholes, the cleanest example of the low-energy manifold of states whose imprint characterizes the topological order is seen in the (particle) entanglement spectrum of a FCI ground state. The particle entanglement spectrum of the ground state reveals the physics of the excitations of the system in the particular topologically ordered state of the ground state. It is more robust than the actual energy spectrum because the latter can exhibit aliasing effects due to other states at nearby fillings. Since the Hamiltonian used to obtain the spectrum is not a "model" Haldane pseudopotential Hamiltonian but a generic Hubbard-like one, adding too many quasiholes to the system can, in the energy spectrum, take us to a state at a different filling (with different quasihole counting). However, the entanglement spectrum will keep the topological order (filling) of the original ground state and reveal directly the quasiholes of that state. For example, if we are looking at the energy spectrum of four particles in 36 orbitals on the lattice, it is possible that instead of seeing the spectrum of four electrons in a 1/3 Abelian state with 24 extra quasiholes, we could, since the interaction is generic Hubbard, obtain the spectrum of four electrons in a filling 1/9 Abelian state or four electrons in a filling 1/7 state with 8 extra quasiholes. However, the particle entanglement spectrum of the ground state with $N = 12$ particles in 36 orbitals (filling 1/3) would reveal the physics of the excitations of an Abelian 1/3 state if we look at the particle entanglement spectrum (described below) of $N_A = 4$ particles versus the rest.

The spectrum of the Chern insulator at 1/3 filling has a quasidegenerate (threefold, as our analysis would imply) ground state, at momenta consistent with the folding rule

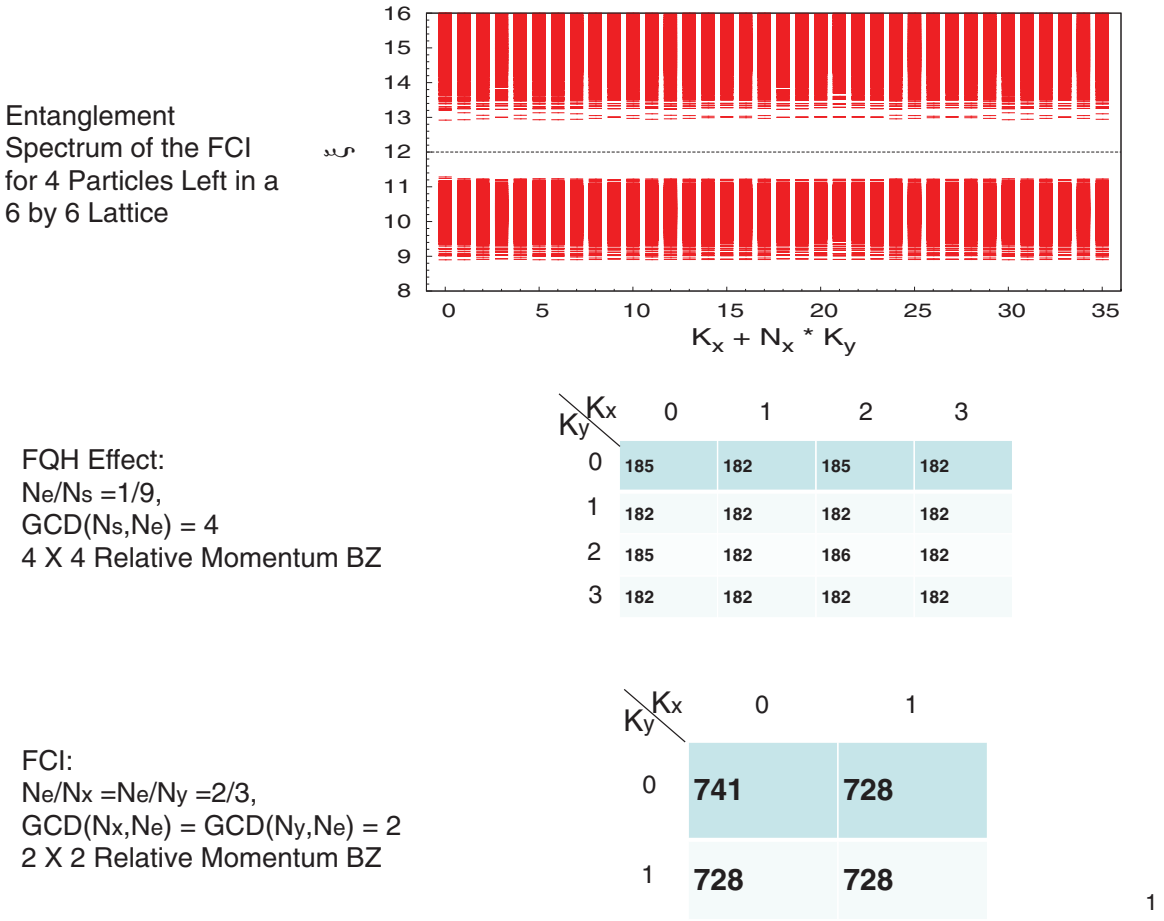

FIG. 4. (Color online) Example of the FQH to FCI mapping for $N_e = 4$, $N_x = 6$, $N_y = 6$. The one-body flat-band Chern Hamiltonian[20] with nearest-neighbor interaction for 12 particles in a 6×6 lattice has a threefold quasidegenerate ground state from which we build the entanglement spectrum shown here. The low-energy manifold (below the dotted line) has 741 states in momentum sectors where $N_x (\mathrm{mod}\, 2) = N_y (\mathrm{mod}\, 2) = 0$ and 728 elsewhere. The counting of the low-energy manifold of states exhibits clear 3×3-fold (in k_x,k_y) center-of-mass degeneracies and the relative momentum BZ of the FCI is a 2×2 BZ. The counting per momentum sector in this BZ is a folding of the counting of zero modes of the Haldane FQH pseudopotential whose highest density state is the Laughlin state. For example, the (0,0) relative momentum sector of the FCI contains 741 states which exactly equals the $p_x/p = p_y/p = 2$ folding $185 + 185 + 185 + 186$ of the FQH Laughlin quasihole counting. Likewise, the (0,1) FCI relative momentum sector contains 728 states, which exactly equals the $p_x/p = p_y/p = 2$ folding $182 + 182 + 182 + 182$ of the FQH Laughlin quasihole counting. This implies that the universality class of the FCI state is the same as that of the $\nu = 1/3$ state.

(we do not expand on this rule for the ground state, as we will give the much more complicated quasihole example). The threefold degenerate ground state of the system contains information about the Abelian fractional 1/3 character of the excitation spectrum. This comes out of the recently developed entanglement spectrum[11,12] which for a single nondegenerated ground state $|\Psi\rangle$ can be defined through the Schmidt decomposition of $|\Psi\rangle$ in two regions A, B (not necessarily spatial):

$$|\Psi\rangle = \sum_i e^{-\xi_i/2} \left|\Psi_i^A\right\rangle \otimes \left|\Psi_i^B\right\rangle, \tag{75}$$

where $\langle\Psi_i^A|\Psi_j^A\rangle = \langle\Psi_i^B|\Psi_j^B\rangle = \delta_{i,j}$. The $\exp(-\xi_i)$ and $|\Psi_i^A\rangle$ are the eigenvalues and eigenstates of the reduced density matrix, $\rho_A = \mathrm{Tr}_B \rho$, where $\rho = |\Psi\rangle\langle\Psi|$ is the total density matrix. There is no generalization of the Schmidt decomposition (75) to degenerate ground states but definition of the entanglement spectrum (ES) through the reduced density matrix still holds. We want to build a density matrix which commutes with the total translation operators, a desirable feature if we want to sort the ξ_i with respect to the momentum quantum numbers. Such a condition is satisfied[11] by the incoherent summation over the degenerate ground states $\rho = \frac{1}{3}\sum_i |\Psi_i\rangle\langle\Psi_i|$. Depending on whether the A and B regions are real, momentum, or particle space, the ES reveals different aspects of the system's excitations. If the regions A, B are regions of particles, it can be proved[11] that the particle ES obtained by tracing over the positions of a set of B particles gives information about the number of quasiholes of the system of N_A particles and the number of orbitals identical to that of the untraced system. In the case of the usual FQH, the particle ES of a model state (such as Laughlin, MR, etc.) contains a number of levels identical to that of the quasiholes, thereby providing a numerical check of our analytic proof.[11] Away from the model states (the Coulomb ground state, for example) the ES may exhibit an entanglement gap.[12,35] It separates a low-energy structure

with perfect quasihole counting and and a high-entanglement energy nonuniversal part. However, a clear and significant gap is not always observed, even for the $\nu = 1/3$ Coulomb state.

Surprisingly, for the FCI, the situation is much better: In a previous work,[8] we observed a clear, large entanglement gap between a manifold of low-entanglement energy levels and a manifold of high-entanglement energy levels. Moreover, the counting of the levels below the gap is identical to the counting of quasiholes of N_A particles in $N_x N_y$ orbitals. We show this for a large-size example. Of the threefold quasidegenerate ground state of 12 particles on the Chern insulator on the checkerboard lattice with $N_x \times N_y = 6 \times 6$, we build the density matrix and construct the ES for $N_A = 4$ particles. The one-body Chern insulator model of Ref. 20 presented in Eq. (78), with a two-body nearest-neighbor Hubbard $U = 1$ interaction in the flat-band limit is used to generate the threefold quasidegenerate ground states. The ES has a gap (see Fig. 4); the counting of the low-energy manifold of states below the dotted line is 741 in momentum sectors where $N_x (\mathrm{mod}\, 2) = N_y (\mathrm{mod}\, 2) = 0$ and 728 elsewhere. The total number below this line (26 325) exactly matches the number of (1,3)-admissible configurations of 4 particles in 36 orbitals. The counting per relative momentum sector is a folding of that of the zero modes in the FQH state, as the complete analysis of Fig. 4 shows.

As said in our previous paper,[8] we find it very revealing that the FCI ground states obtained here contain much clearer information (large, clear entanglement gap) than the ground states of the Coulomb interaction in the FQH. The ES shows that the ground states by themselves know of the fractional nature of the excitations in the FCI. The current clean application of the ES also shows that this quantity is fundamentally useful toward revealing the physics of strongly correlated states besides the usual FQH model wave functions. This is even crucial in this case since, despite several attempts,[36,37] there is no analytical expression of the Laughlin state for the FCI to compare with.

V. NUMERICAL PROOF OF EMERGENT SYMMETRIES IN ABELIAN AND NON-ABELIAN FRACTIONAL CHERN INSULATORS

In the current section, we expand our numerical analysis of FCI states to the non-Abelian case and show that the counting rule obtained in the current analysis is robust. We perform exhaustive numerical calculations of both the energy and the entanglement spectra for several interactions at the specific filling where non-Abelian states are expected. The calculations serve as both a numerical check of our emergent translational symmetry principle, as well as the first proof of principle that non-Abelian states can be stabilized in a fractionally filled Chern insulator.

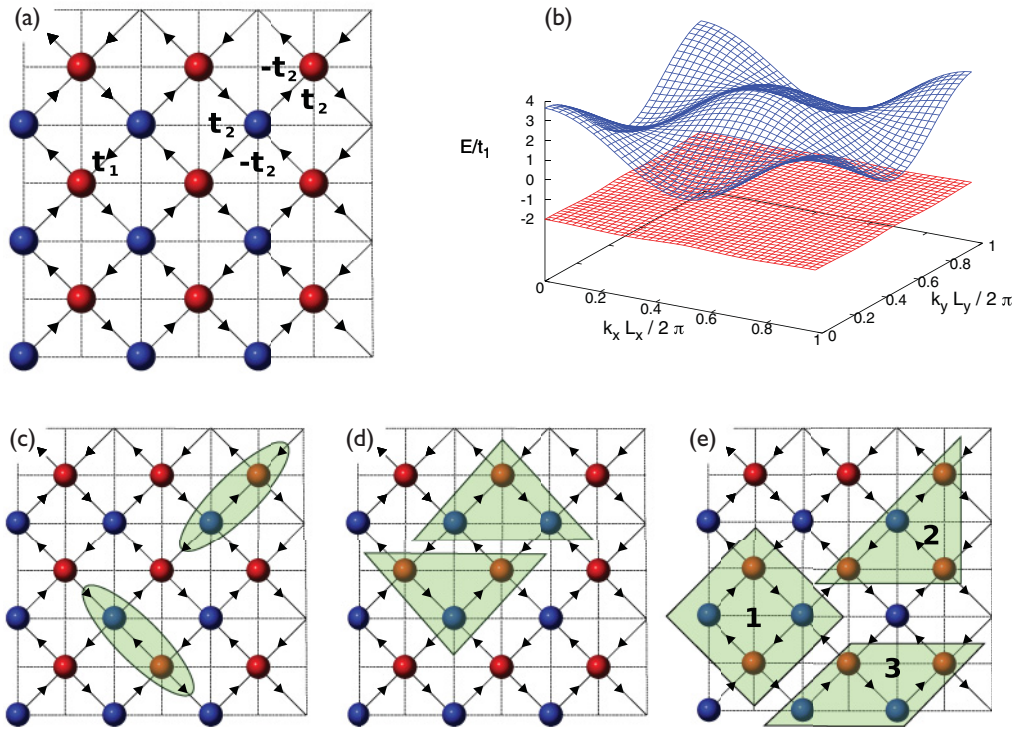

FIG. 5. (Color online) (a) One-body model hopping amplitudes in the checkerboard Chern insulator model used in our numerical calculations. Direction of the arrow means positive hopping amplitude. (b) Dispersion of the model shows that it is an insulator with a nearly flat valence band. Our diagonalizations are in the flat-band limit where the valence band is made completely flat. (c) Simplest Hubbard two-body interaction couples nearest-neighbor sites used to obtain the Abelian 1/3 state. (d) Simplest three-body Hubbard interaction used to obtain the non-Abelian MR Pfaffian state. Equal weight is given to the three configurations. (e) Simplest four-body Hubbard interaction configurations used to obtain the non-Abelian $\mathbb{Z}_3$ RR states. Any of the interactions 1,2,3 can be used, all giving a RR ground state but of different gaps (the largest gap being obtained with interaction 1).

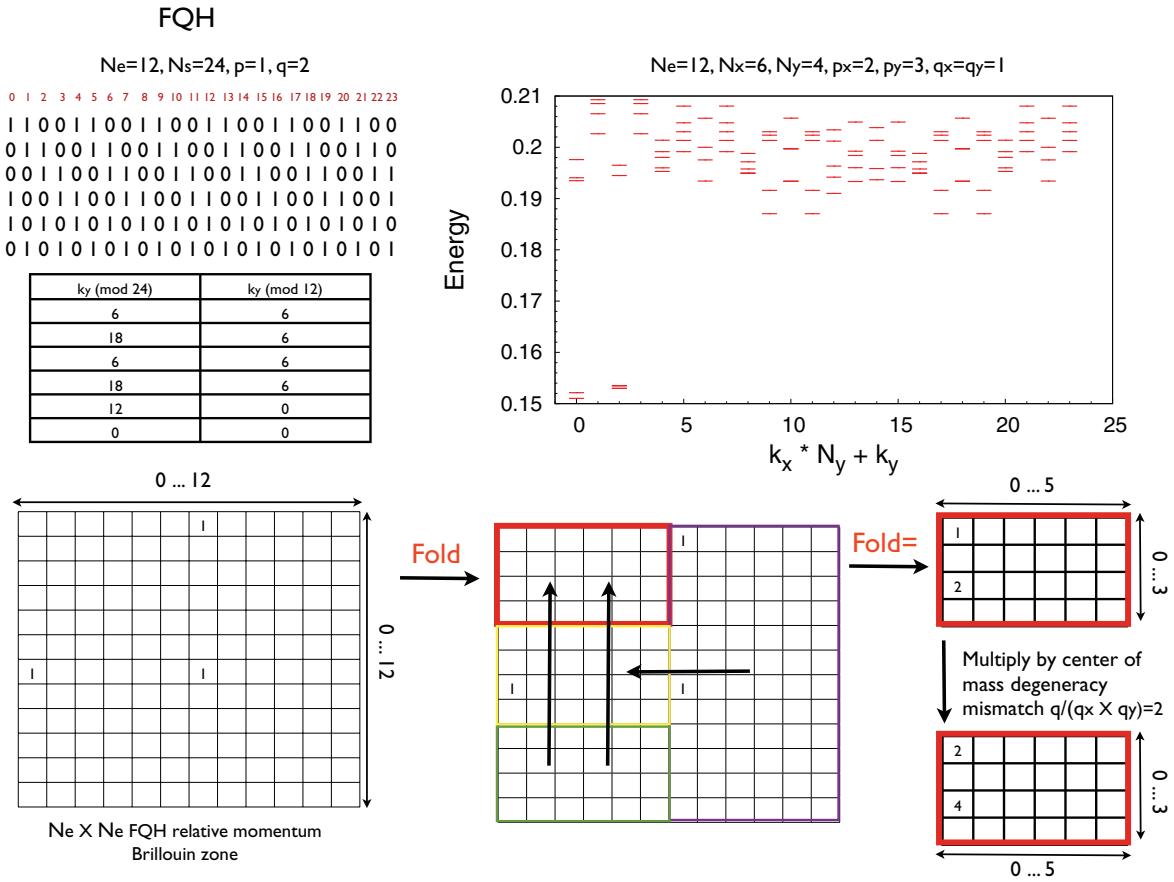

FIG. 6. (Color online) The spectrum of the three-body Hubbard interaction at filling $\nu = 1/2$ shows two quasidegenerate states at (0,0) momentum and four states (separated into two quasidegenerate doublets) at (0,2) (in units of the smallest lattice momentum). The procedure and folding from FQH to FCI are also presented.

For our one-body model, we pick the Chern insulator on a checkerboard lattice, first introduced in Refs. 9, 10, and 20. This model already exhibits weak dispersion of the bands (see Fig. 5) like several other models.[38–40] However, because we work in the flat-band limit, this is not essential to our calculation. With A,B being the two sites in the unit cell, the one-body, two-band Hamiltonian reads[20]

$$H_1 = \sum_k (c^\dagger_{kA}, c^\dagger_{kB}) h_1(k) (c_{kA}, c_{kB})^T, \quad h_1(k) = \sum_i d_i(k)\sigma_i, \tag{76}$$

where the $d_i(k)$'s are

$$\begin{aligned} d_x(k) &= 4t_1 \cos(\phi)\cos(k_x/2)\cos(k_y/2), \\ d_y(k) &= 4t_1 \sin(\phi)\sin(k_x/2)\sin(k_y/2), \\ d_z &= 2t_2[\cos(k_x) - \cos(k_y)] + M \end{aligned} \tag{77}$$

In the original model[20] there is an additional diagonal term—$4t_3\cos(k_x)\cos(k_y)$—which shrinks the dispersion of the bands, thereby making them flatter, but does not matter for the eigenstates; since we are diagonalizing in the flat-band limit, we neglect such a term. ϕ is the phase factor added to the nearest-neighbor hopping, while the parameter M is a mass term added in order to drive the transition from a topological Chern insulator (for $M = 0$) to a trivial atomic limit insulator when $M \to \pm\infty$. The model is always gapped (for t_1, t_2, ϕ not vanishing) with the exception of the points $k_x = 0$, $k_y = \pi$, $M = -4t_2$ and $k_x = \pi$, $k_y = 0$, $M = 4t_2$, which are gapless and where the phase transitions between the atomic limits $M \to \pm\infty$ and the Chern insulator phase occur. For $|M| < 4|t_2|$ the filled valence band has a Hall conductance of 1. The single-particle Hamiltonian matrix has the following symmetries: inversion with identity inversion matrix $h_1(-k_x,-k_y) = h_1(k_x,k_y)$, as well as (at $M = 0$) a certain type of particle-hole symmetry coupled with a C_4 rotation and a mirror operation: $\sigma_z h_1(k_x,k_y)\sigma_z = -h_1(k_y,k_x)$. Due to the presence of fractions $k/2$, the model in Ref. 20 is not in Bloch form. To render it in Bloch form, we perform the gauge transformation $c_{kB} \to c_{kB}\exp[-i(k_x - k_y)/2]$ to obtain

$$\begin{aligned} h_2(k) &= \begin{pmatrix} h_{11}(k) & h_{12}(k) \\ h^\star_{12}(k) & -h_{11}(k) \end{pmatrix}, \\ h_{12}(k) &= t_1 e^{i\phi}(1 + e^{i(k_y - k_x)}) + t_1 e^{-i\phi}(e^{ik_y} + e^{-ik_x}), \\ h_{11}(k) &= 2t_2[\cos(k_x) - \cos(k_y)] + M. \end{aligned} \tag{78}$$

The inversion symmetry of $h_1(k)$ translates into a symmetry of $h_2(k)$ given by $U^\dagger(k)h_2(\vec{k})U(k) = h_2(-\vec{k})$ with $U(k)$ a diagonal 2×2 unitary matrix with $1, e^{-i(k_x - k_y)/2}$ on the diagonal. To eliminate the effect of the band curvature, and to allow the filled particles to democratically sample the whole BZ, we always work in the flat-band limit of a topological

insulator. This corresponds to keeping the single-particle eigenstates of $h_2(k)$ but putting the energy of the occupied bands to be an arbitrary energy $\pm E_0$, where $E_0 > 0$. At the Hamiltonian level, we transform from $h_2(k) = E_-(k)P_-(k) + E_+(k)P_+(k)$ to $h_2^{FB}(k) = -E_0 P_-(k) + E_0 P_+(k)$, where $P_\pm$ are the projectors onto the occupied and unoccupied bands. The energy difference between the valence and conduction bands can hence be made large without changing the eigenstates of the system.

We now fractionally fill the flat valence band of this insulator and add interactions. We diagonalize the interaction Hamiltonian directly in the filled band, neglecting the conduction band. This is similar to the LLL projection in the usual FQH Effect. Several interactions we use are

$$H_{\text{two-body}} = \sum_{\langle AB\rangle} n_A n_B, \tag{79}$$

where A,B are nearest-neighbor A,B sites. In the current section we also use other many-body interactions such as three-body:

$$H_{\text{three-body}} = \sum_{\langle AB_1\rangle,\langle A,B_2\rangle} n_A n_{B_1} n_{B_2} + n_B n_{A_1} n_{A_2}, \tag{80}$$

where B_1, B_2 are the two nearest neighbors of the site A and A_1, A_2 are the two nearest neighbors of the site B. The first of the three kinds of four-body interactions used in our exact diagonalization reads (see Fig. 5):

$$H_{\text{four-body 1}} = \sum_{\langle A_1,B_1\rangle,\langle A_1,B_2\rangle,\langle\langle A_1,A_2\rangle\rangle,\langle\langle B_1,B_2\rangle\rangle} n_{A_1} n_{A_2} n_{B_1} n_{B_2}, \tag{81}$$

where B_1, B_2 are the two nearest neighbors of the sites A_1 and also of the site A_2. The other two four-body interactions used which we denote $H_{\text{four-body 2}}$, $H_{\text{four-body 3}}$ can be easily understood from Fig. 5. All the numerical calculations are performed with $t_2 = (2-\sqrt{2})/2t_1$, as discussed in Ref. 20. The total translation operators in the x,y directions commute with both the single- and many-body Hamiltonian and hence the eigenstates are indexed by total momentum quantum numbers (K_x, K_y) which are the sum of the momentum quantum numbers of each of the N particles modulo (N_x, N_y). The basis states are $\prod_{i=1}^{N} \gamma^\dagger_{-,\vec{k}_1} \ldots \gamma^\dagger_{-,\vec{k}_N} |0\rangle$ (we work in the LLL and the $\gamma^\dagger_{-,\vec{k}}$'s are the creation operators for a particle of momentum $\vec{k}$ in the valence band). When acting on the basis states, the $c_{\vec{k},\alpha} = u_{-,\alpha,\vec{k}} \gamma_{-,\vec{k}}$, where $u_{-,\alpha,\vec{k}}$ is the $\alpha = A,B$ component of the eigenstate of the occupied band of $h_2(k)$ or $h_2^{FB}(k)$ (they have identical eigenstates). Diagonalizing directly in the valence band provides for large numerical efficiency, allowing us to go to very large system sizes. The inversion symmetry of the single-particle problem is maintained at the interacting level, and the interacting spectrum has an exact $(K_x, K_y) \to (-K_x, -K_y)$ symmetry which can and has been used as a checkup. The $H_{\text{two-body}}$ has been used to obtain the Abelian, filling 1/3 FCI topological state.

We now use $H_{\text{three-body}}$ and, borrowing from FQH experience, we look for the MR Pfaffian at filling $\nu = 1/2$. We diagonalize $H_{\text{three-body}}$ for up to $N = 14$ particles on a $N_x \times N_y = 7 \times 4$ lattice and present the spectrum in Fig. 6.

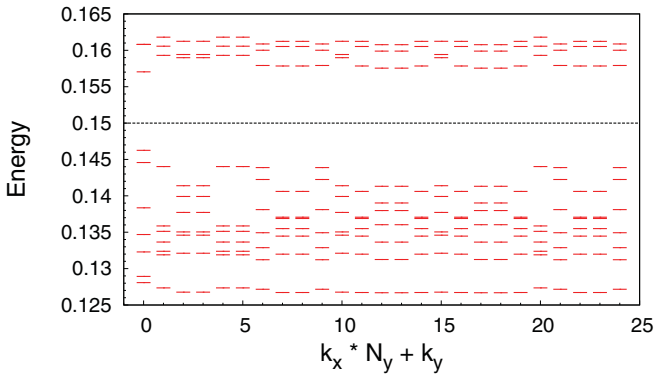

FIG. 7. (Color online) Low-lying spectrum of the three-body interaction for $N_e = 12$ electrons and $N_x = N_y = 5$.

The spectrum is separated into a sixfold quasidegenerate ground state [at momentum (0,2) we have four states, separated into two exactly degenerate doublets] at momenta consistent with our FQH to FCI mapping (in this case we also have to use the center-of-mass degeneracy mismatch factor, which is 2). A clear and detailed presentation of the resolution of states in momentum sectors is shown in Fig. 6. Both the number of ground states and their momenta are consistent with the MR Pfaffian state, with a large gap separation to the continuum of states. We now add quasiholes to the system, by performing the diagonalization of the three-body Hamiltonian for $N_e = 12$ electrons on a $N_x \times N_y = 5 \times 5$ lattice. This represents the addition of one flux quantum to the system. The spectrum is seen in Fig. 7, and we observe a low-energy manifold of states (below the dashed line) with 7 states in each momentum sector separated by a clear energy gap from a high-energy continuum of states. This is indeed the correct counting for the non-Abelian quasiholes of the MR state based on our emergent symmetry principle. We then close the analysis of the MR state by looking at the particle ES of the $N_e = 14, N_x = 7, N_y = 4$ degenerate states when the number of particles not traced out of the system is $N_A = 6$. By our theory, this spectrum should show the counting, per momentum sector, in a low-energy

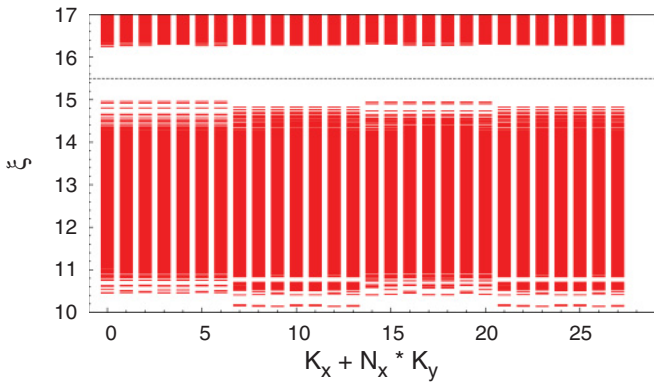

FIG. 8. (Color online) Entanglement spectrum for the ground states of the three-body interaction for $N_e = 14$ electrons and $N_x = 7, N_y = 4$, and $N_A = 6$ particles. The number of states per momentum sector below the dotted line is 8463 in the even k_y sectors and 8486 in the odd k_y sectors. This is the counting predicted by our FQH to FCI mapping.

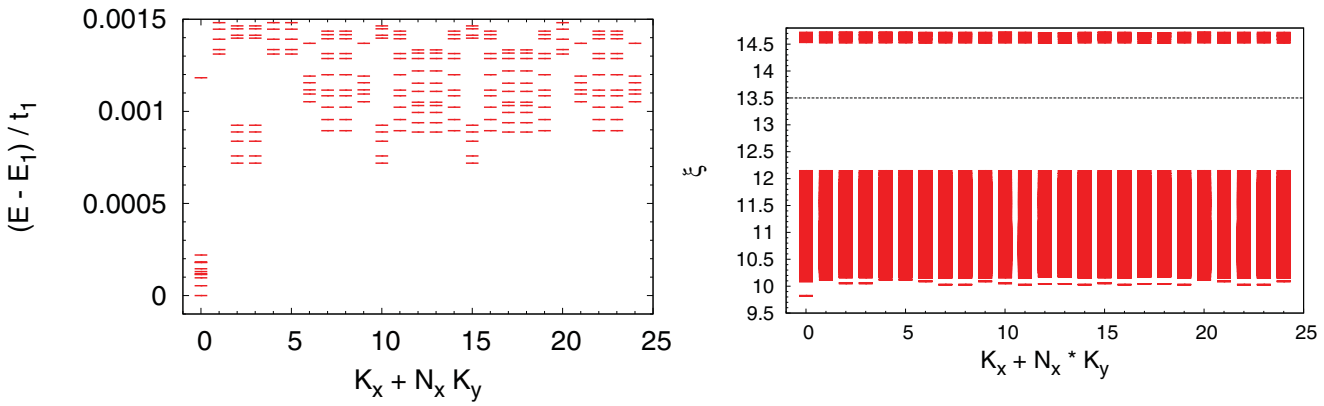

FIG. 9. (Color online) (Left) Low-lying spectrum of the four-body interaction for $N_e = 15$ electrons and $N_x = N_y = 5$. The ground-state manifold is made of the 10 low-energy states in the $(k_x = 0, k_y = 0)$ sector. (Right) Entanglement spectrum for the ground states of the four-body interaction for $N_e = 15$ electrons and $N_x = N_y = 5$ and $N_A = 5$ particles. The number of states per momentum sector below the dotted line is 2050, except in the $(k_x = 0, k_y = 0)$ sector, which has 2055 states. This is the correct counting predicted by our FQH to FCI mapping.

manifold of the quasiholes of the MR state for 6 particles in 28 orbitals. The results are presented in Fig. 8, where we again see that a low-lying manifold of states is separated by a gap form a manifold of spurious continuum. The number of states per momentum sector below the dotted line in Fig. 8 is 8463 in the even k_y sectors and 8486 in the odd k_y sectors, the correct numbers of non-Abelian quasiholes predicted by our FQH to FCI mapping.

We conclude that we have presented sufficient proof that the FCI state at half filling with three-body potential is of MR type in the FCI. We now move to the four-body interaction. The $\mathbb{Z}_3$ RR state occurs at filling factor 3/5. We have performed the calculations up to $N = 15$. Figure 9 shows the energy spectrum for $N = 15$ with a lattice size $N_x = N_y = 5$. We see a tenfold low-energy manifold at momenta consistent with our FQH to FCI mapping, clearly separated from the higher-energy continuum. The particle ES of this ground-state manifold is given in Fig. 9. While all N_A sectors display a full entanglement gap, we have chosen the $N_A = 5$ sector. This case exhibits an identical counting (2050 states) in all momentum sectors except in the $(k_x = 0, k_y = 0)$ sector, where the counting is 2055. Once again, this result is in agreement with our FQH to FCI mapping.

VI. CONCLUSIONS

In this paper, we have explained the emergent translational symmetry apparent in the low-energy manifold of states of a fractionally filled Chern insulator when the insulator exhibits a topologically ordered state. We have shown that the one-body GMP algebra obtained at long wavelength in Ref. 15 maps the problem of a Chern insulator on a $N_x \times N_y$ lattice in the problem of a FQH state in the LLL with number of fluxes $N_s = N_x N_y$ piercing the torus and with a periodic background potential superimposed on the many-body potential already present in the system. We revisited the continuum FQH problem and presented a detailed derivation of the many-body relative translational symmetries in the system (after the center-of-mass motion is taken out) presented in a classic paper by Haldane.[19] We then showed that the BZ of the FCI is just a folding of the one for the FQH and pointed out the direct connection between the center-of-mass degeneracies in the FCI and those in the FQH. This FQH-FCI map allows us to compute the number of states that arise per momentum sector of the FCI *if the FCI is in the same topological phase as the FQH*. We showed how to obtain, in the FQH effect, the counting of quasihole states per two-dimensional relative momentum sector for a large series of states exhibiting a generalized Pauli principle.[21] These states include the Laughlin, MR, and RR series, as well as the Jack polynomial states, the Haffnian,[41] and many others, including extensions to spin-unpolarized states.[42,43] The counting construction makes use of only combinatoric methods and involves counting partitions. We showed how to use the combinatoric counting rule and the FQH-FCI map to obtain the number of states per momentum sector in both the energy and the entanglement spectra of the FCI at filling 1/3. We then proceeded on a comprehensive numerical analysis of the spectra of Chern insulators with three- and four-body interactions. We provided a proof of principle that MR states and RR $\mathbb{Z}_3$ non-Abelian states can be stabilized in Chern insulators and provided a numerical check of our FQH-FCI mapping.

ACKNOWLEDGMENTS

B. A. B. wishes to thank Z. Papic, F. D. M. Haldane, T. L. Hughes, S. Sondhi, and S. A. Parameswaran for useful discussions. B. A. B. was supported by Princeton Startup Funds, NSF CAREER DMR-095242, ONR-N00014-11-1-0635, Darpa-N66001-11-1-4110, and NSF-MRSEC DMR-0819860 at Princeton University. B. A. B. thanks Technion, Israel, and Ecole Normale Superieure, Paris, for generous hosting during the stages of this work.

APPENDIX A: DETAILS OF THE GIRVIN-MACDONALD-PLATZMAN ALGEBRA

In this Appendix, we prove in detail that

$$\sum_{n_2} u^{n_1\star}_{\alpha,k} u^{n_2}_{\alpha,k+q} u^{n_2\star}_{\beta,k+q} u^{m_2}_{\beta,k+w+q} - u^{n_1\star}_{\beta,k} u^{n_2}_{\beta,k+w} u^{n_2\star}_{\alpha,k+w} u^{m_2}_{\alpha,k+w+q} \approx \frac{i}{2}(q_i w_j - w_i q_j) F^{n_1 m_2}_{ij}. \quad \text{(A1)}$$

The expansion (double index means summation)

$$u^{n}_{\alpha,k+q} = u^{n}_{\alpha,k} + q_i\partial_i u^{n}_{\alpha,k} + \tfrac{1}{2}q_iq_j\partial_i\partial_j u^{n}_{\alpha,k} \tag{A2}$$

gives

$$\begin{aligned}
&u^{n_1\star}_{\alpha,k}\big(u^{n_2}_{\alpha,k} + q_i\partial_i u^{n_2}_{\alpha,k} + \tfrac{1}{2}q_iq_j\partial_i\partial_j u^{n_2}_{\alpha,k}\big)\big(u^{n_2\star}_{\beta,k} + q_i\partial_i u^{n_2\star}_{\beta,k} + \tfrac{1}{2}q_iq_j\partial_i\partial_j u^{n_2\star}_{\beta,k}\big)\big[u^{m_2}_{\beta,k} + (q_i+w_i)\partial_i u^{m_2}_{\beta,k}\\
&\quad + \tfrac{1}{2}(q_i+w_i)(q_j+w_j)\partial_i\partial_j u^{m_2}_{\beta,k}\big] - u^{n_1\star}_{\beta,k}\big(u^{n_2}_{\beta,k} + w_i\partial_i u^{n_2}_{\beta,k} + \tfrac{1}{2}w_iw_j\partial_i\partial_j u^{n_2}_{\beta,k}\big)\big(u^{n_2\star}_{\alpha,k} + w_i\partial_i u^{n_2\star}_{\alpha,k} + \tfrac{1}{2}w_iw_j\partial_i\partial_j u^{n_2\star}_{\alpha,k}\big)\\
&\quad\times\big[u^{m_2}_{\alpha,k} + (q_i+w_i)\partial_i u^{m_2}_{\alpha,k} + \tfrac{1}{2}(q_i+w_i)(q_j+w_j)\partial_i\partial_j u^{m_2}_{\alpha,k}\big]\\
&= \big(\delta_{n_1,n_2} + q_iu^{n_1\star}_{\alpha,k}\partial_i u^{n_2}_{\alpha,k} + \tfrac{1}{2}q_iq_ju^{n_1\star}_{\alpha,k}\partial_i\partial_j u^{n_2}_{\alpha,k}\big)\cdot\big(\delta_{n_2,m_2} + (q_i+w_i)u^{n_2\star}_{\beta,k}\partial_i u^{m_2}_{\beta,k}\\
&\quad + \tfrac{1}{2}(q_i+w_i)(q_j+w_j)u^{n_2\star}_{\beta,k}\partial_i\partial_j u^{m_2}_{\beta,k} + q_iu^{m_2}_{\beta,k}\partial_i u^{n_2\star}_{\beta,k} + q_i(q_j+w_j)\big(\partial_i u^{n_2\star}_{\beta,k}\big)\big(\partial_j u^{m_2}_{\beta,k}\big) + \tfrac{1}{2}q_iq_ju^{m_2}_{\beta,k}\partial_i\partial_j u^{n_2\star}_{\beta,k}\big)\\
&\quad - \big(\delta_{n_1,n_2} + w_iu^{n_1\star}_{\beta,k}\partial_i u^{n_2}_{\beta,k} + \tfrac{1}{2}w_iw_ju^{n_1\star}_{\beta,k}\partial_i\partial_j u^{n_2}_{\beta,k}\big)\cdot\big[\delta_{n_2,m_2} + (q_i+w_i)u^{n_2\star}_{\alpha,k}\partial_i u^{m_2}_{\alpha,k}\\
&\quad + \tfrac{1}{2}(q_i+w_i)(q_j+w_j)u^{n_2\star}_{\alpha,k}\partial_i\partial_j u^{m_2}_{\alpha,k} + w_iu^{m_2}_{\alpha,k}\partial_i u^{n_2\star}_{\alpha,k} + w_i(q_j+w_j)\big(\partial_i u^{n_2\star}_{\alpha,k}\big)\big(\partial_j u^{m_2}_{\alpha,k}\big) + \tfrac{1}{2}w_iw_ju^{m_2}_{\alpha,k}\partial_i\partial_j u^{n_2\star}_{\alpha,k}\big]\\
&= \delta_{n_1,m_2} + (q_i+w_i)u^{n_1\star}_{\beta,k}\partial_i u^{m_2}_{\beta,k} + \tfrac{1}{2}(q_i+w_i)(q_j+w_j)u^{n_1\star}_{\beta,k}\partial_i\partial_j u^{m_2}_{\beta,k} + q_iu^{m_2}_{\beta,k}\partial_i u^{n_1\star}_{\beta,k} + q_i(q_j+w_j)\big(\partial_i u^{n_1\star}_{\beta,k}\big)\big(\partial_j u^{m_2}_{\beta,k}\big)\\
&\quad + \tfrac{1}{2}q_iq_ju^{m_2}_{\beta,k}\partial_i\partial_j u^{n_1\star}_{\beta,k} + q_iu^{n_1\star}_{\alpha,k}\partial_i u^{m_2}_{\alpha,k} + q_j(q_i+w_i)u^{n_1\star}_{\alpha,k}\big(\partial_j u^{n_2}_{\alpha,k}\big)u^{n_2\star}_{\beta,k}\partial_i u^{m_2}_{\beta,k} + q_jq_iu^{n_1\star}_{\alpha,k}\big(\partial_j u^{n_2}_{\alpha,k}\big)u^{m_2}_{\beta,k}\partial_i u^{n_2\star}_{\beta,k}\\
&\quad + \tfrac{1}{2}q_iq_ju^{n_1\star}_{\alpha,k}\partial_i\partial_j u^{m_2}_{\alpha,k} - (q\leftrightarrow w,\alpha\leftrightarrow\beta).
\end{aligned} \tag{A3}$$

The zeroth-order term in q cancels. We now group the first- and second-order terms. The first-order terms are

$$\begin{aligned}
&(q_i+w_i)u^{n_1\star}_{\beta,k}\partial_i u^{m_2}_{\beta,k} + q_i\big(u^{m_2}_{\beta,k}\partial_i u^{n_1\star}_{\beta,k} + u^{n_1\star}_{\alpha,k}\partial_i u^{m_2}_{\alpha,k}\big) - (q\leftrightarrow w,\alpha\leftrightarrow\beta)\\
&\quad = (q_i+w_i)u^{n_1\star}_{\beta,k}\partial_i u^{m_2}_{\beta,k} + q_i\partial_i\big(u^{m_2}_{\beta,k}u^{n_1\star}_{\beta,k}\big) - (q\leftrightarrow w,\alpha\leftrightarrow\beta)\\
&\quad = (q_i+w_i)u^{n_1\star}_{\beta,k}\partial_i u^{m_2}_{\beta,k} - (q\leftrightarrow w,\alpha\leftrightarrow\beta) = 0
\end{aligned} \tag{A4}$$

(summation over α,β was implied). Hence, the first-order term is zero.

The second-order term is (remember double index summation):

$$\begin{aligned}
&\tfrac{1}{2}(q_i+w_i)(q_j+w_j)u^{n_1\star}_{\beta,k}\partial_i\partial_j u^{m_2}_{\beta,k} + q_i(q_j+w_j)\big(\partial_i u^{n_1\star}_{\beta,k}\big)\big(\partial_j u^{m_2}_{\beta,k}\big) + \tfrac{1}{2}q_iq_ju^{m_2}_{\beta,k}\partial_i\partial_j u^{n_1\star}_{\beta,k}\\
&\quad + q_j(q_i+w_i)u^{n_1\star}_{\alpha,k}\big(\partial_j u^{n_2}_{\alpha,k}\big)u^{n_2\star}_{\beta,k}\partial_i u^{m_2}_{\beta,k} + q_jq_iu^{n_1\star}_{\alpha,k}\big(\partial_j u^{n_2}_{\alpha,k}\big)u^{m_2}_{\beta,k}\partial_i u^{n_2\star}_{\beta,k} + \tfrac{1}{2}q_iq_ju^{n_1\star}_{\alpha,k}\partial_i\partial_j u^{m_2}_{\alpha,k} - (q\leftrightarrow w,\alpha\leftrightarrow\beta)\\
&= [q_i(q_j+w_j) - w_i(q_j+w_j)]\big(\partial_i u^{n_1\star}_{\beta,k}\big)\big(\partial_j u^{m_2}_{\beta,k}\big) + \tfrac{1}{2}(q_iq_j - w_iw_j)u^{m_2}_{\beta,k}\partial_i\partial_j u^{n_1\star}_{\beta,k}\\
&\quad + q_j(q_i+w_i)u^{n_1\star}_{\alpha,k}\big(\partial_j u^{n_2}_{\alpha,k}\big)u^{n_2\star}_{\beta,k}\partial_i u^{m_2}_{\beta,k} - w_j(q_i+w_i)u^{n_1\star}_{\beta,k}\big(\partial_j u^{n_2}_{\beta,k}\big)u^{n_2\star}_{\alpha,k}\partial_i u^{m_2}_{\alpha,k}\\
&\quad + q_jq_iu^{n_1\star}_{\alpha,k}\big(\partial_j u^{n_2}_{\alpha,k}\big)u^{m_2}_{\beta,k}\partial_i u^{n_2\star}_{\beta,k} - w_jw_iu^{n_1\star}_{\beta,k}\big(\partial_j u^{n_2}_{\beta,k}\big)u^{m_2}_{\alpha,k}\partial_i u^{n_2\star}_{\alpha,k} + \tfrac{1}{2}(q_iq_j - w_iw_j)u^{n_1\star}_{\alpha,k}\partial_i\partial_j u^{m_2}_{\alpha,k}\\
&= (q_iw_j - w_iq_j)\big[\big(\partial_i u^{n_1\star}_{\beta,k}\big)\big(\partial_j u^{m_2}_{\beta,k}\big) - u^{n_1\star}_{\alpha,k}\big(\partial_j u^{n_2}_{\alpha,k}\big)u^{n_2\star}_{\beta,k}\partial_i u^{m_2}_{\beta,k}\big]\\
&\quad + \tfrac{1}{2}(q_iq_j - w_iw_j)\big[u^{m_2}_{\beta,k}\partial_i\partial_j u^{n_1\star}_{\beta,k} + u^{n_1\star}_{\alpha,k}\partial_i\partial_j u^{m_2}_{\alpha,k} + 2\big(\partial_i u^{n_1\star}_{\beta,k}\big)\big(\partial_j u^{m_2}_{\beta,k}\big)\big]\\
&\quad + q_iq_j\big[u^{n_1\star}_{\alpha,k}\big(\partial_j u^{n_2}_{\alpha,k}\big)u^{m_2}_{\beta,k}\partial_i u^{n_2\star}_{\beta,k} + u^{n_1\star}_{\alpha,k}\big(\partial_j u^{n_2}_{\alpha,k}\big)u^{n_2\star}_{\beta,k}\partial_i u^{m_2}_{\beta,k}\big] - w_iw_j\big[u^{n_1\star}_{\beta,k}\big(\partial_j u^{n_2}_{\beta,k}\big)u^{m_2}_{\alpha,k}\partial_i u^{n_2\star}_{\alpha,k} + u^{n_1\star}_{\beta,k}\big(\partial_j u^{n_2}_{\beta,k}\big)u^{n_2\star}_{\alpha,k}\partial_i u^{m_2}_{\alpha,k}\big].
\end{aligned} \tag{A5}$$

We now observe several simplifications. The last line of the above equation vanishes due to the identity

$$u^{n_1\star}_{\alpha,k}\big(\partial_j u^{n_2}_{\alpha,k}\big)u^{m_2}_{\beta,k}\partial_i u^{n_2\star}_{\beta,k} + u^{n_1\star}_{\alpha,k}\big(\partial_j u^{n_2}_{\alpha,k}\big)u^{n_2\star}_{\beta,k}\partial_i u^{m_2}_{\beta,k} = u^{n_1\star}_{\alpha,k}\big(\partial_j u^{n_2}_{\alpha,k}\big)\partial_i\big(u^{m_2}_{\beta,k}u^{n_2\star}_{\beta,k}\big) = 0. \tag{A6}$$

The second but last line of Eq. (A5) also cancels because of the identity

$$A_{ij}\big[u^{m_2}_{\beta,k}\partial_i\partial_j u^{n_1\star}_{\beta,k} + u^{n_1\star}_{\alpha,k}\partial_i\partial_j u^{m_2}_{\alpha,k} + 2\big(\partial_i u^{n_1\star}_{\beta,k}\big)\big(\partial_j u^{m_2}_{\beta,k}\big)\big] = A_{ij}\partial_i\partial_j\big(u^{m_2}_{\beta,k}u^{n_2\star}_{\beta,k}\big) = 0, \tag{A7}$$

when A_{ij} is any symmetric matrix. We are left with

$$\begin{aligned}
&\sum_{n_2} u^{n_1\star}_{\alpha,k}u^{n_2}_{\alpha,k+q}u^{n_2\star}_{\beta,k+q}u^{m_2}_{\beta,k+w+q} - u^{n_1\star}_{\beta,k}u^{n_2}_{\beta,k+w}u^{n_2\star}_{\alpha,k+w}u^{m_2}_{\alpha,k+w+q}\\
&\quad\approx (q_iw_j - w_iq_j)\big[\big(\partial_i u^{n_1\star}_{\beta,k}\big)\big(\partial_j u^{m_2}_{\beta,k}\big) - u^{n_1\star}_{\alpha,k}\big(\partial_j u^{n_2}_{\alpha,k}\big)u^{n_2\star}_{\beta,k}\partial_i u^{m_2}_{\beta,k}\big]\\
&\quad = \tfrac{1}{2}(q_iw_j - w_iq_j)\big[\big(\partial_i u^{n_1\star}_{\beta,k}\big)\big(\partial_j u^{m_2}_{\beta,k}\big) - u^{n_1\star}_{\alpha,k}\big(\partial_j u^{n_2}_{\alpha,k}\big)u^{n_2\star}_{\beta,k}\partial_i u^{m_2}_{\beta,k} - (i\leftrightarrow j)\big].
\end{aligned} \tag{A8}$$

By denoting the non-Abelian Berry potential

$$A_j^{n_1,n_2} = i u_{\beta k}^{n_1 \star} \partial_j u_\beta^{m_2}, \tag{A9}$$

we find that

$$\begin{aligned}&\left(\partial_i u_{\beta,k}^{n_1 \star}\right)\left(\partial_j u_{\beta,k}^{m_2}\right) - u_{\alpha,k}^{n_1 \star}\left(\partial_j u_{\alpha,k}^{n_2}\right) u_{\beta,k}^{n_2 \star} \partial_i u_{\beta,k}^{m_2} - (i \leftrightarrow j) \\ &\quad = -i F_{ij}^{n_1,n_2}, \end{aligned} \tag{A10}$$

where $F_{ij}^{n_1,n_2} = \partial_i A_j^{n_1,n_2} - \partial_j A_i^{n_1,n_2} - i[A_i, A_j]^{n_1,n_2}$.

APPENDIX B: RELATION BETWEEN THE DENSITY ALGEBRAS AND CHERN NUMBER

The projected densities in the commutator algebra in Eq. (60) are required to not commute if the topological insulator is to have a nonzero Chern number. Taking the trace of the commutator in Eq. (60) with the $\rho_{-q-w} = \frac{1}{\sqrt{N_s}} \sum_k u_{\alpha k-q-w}^{m_1} u_{\alpha k}^{n_2 \star} \gamma_k^{n_2 \dagger} |0\rangle \langle 0| \gamma_{k-q-w}^{m_1}$ we obtain, to second order in q, w (in the long-wavelength limit),

$$\begin{aligned}&[\rho_q, \rho_w]\rho_{-q-w} \\ &\quad = -\frac{i}{2}(q_i w_j - w_i q_j) \frac{1}{N_s^{3/2}} \sum_{k,n_1 m_2} F_{ij}^{n_1,m_2}(k) \gamma_k^{n_1 \dagger} |0\rangle \langle 0| \gamma_k^{m_2}, \end{aligned} \tag{B1}$$

where we have used the fact that $u_{\alpha k-q-w}^{m_1} u_{\alpha k}^{n_2 \star} = \delta_{m_1,n_2}$ to zeroth order in q, w:

$$\begin{aligned}&[\rho_{q_x \hat{x}}, \rho_{w_y \hat{y}}]\rho_{-q_x \hat{x} - w_y \hat{y}} \\ &\quad = \frac{i}{2} q_x w_y \frac{1}{N_s^{3/2}} \sum_{k,n_1 m_2} F_{xy}^{n_1,m_2}(k) \gamma_k^{n_1 \dagger} |0\rangle \langle 0| \gamma_k^{m_2}. \end{aligned} \tag{B2}$$

We now take the trace of the above to obtain

$$\frac{2}{i} \frac{\sqrt{N_s}}{q_x w_y} \mathrm{Tr}([\rho_{q_x \hat{x}}, \rho_{w_y \hat{y}}]\rho_{-q_x \hat{x} - w_y \hat{y}}) = \frac{1}{N_s} \sum_{k,m} F_{xy}^{m,m}(k) = C, \tag{B3}$$

with $q_x = \frac{2\pi}{N_x}$, $q_y = \frac{2\pi}{N_y}$ the lowest value for the momenta one can obtain on the lattice. Hence, the Chern number can be expressed as the long-wavelength limit of the commutator of the projected density operators in the lower sub-band.

APPENDIX C: RELATION BETWEEN THE POSITION OPERATORS AND THE CHERN NUMBER

An alternative way of presenting this result is by using the position operator in the X direction:

$$X = \frac{1}{\sqrt{N_s}} \sum_{j,\alpha} e^{i \Delta q j} |j,\alpha\rangle \langle j,\alpha| = \frac{1}{\sqrt{N_s}} \sum_k c_{k\alpha} |0\rangle \langle 0| c_{k+\Delta q \alpha}, \tag{C1}$$

where by $\Delta k j$ we mean $\Delta \vec{k} \cdot \vec{j}$. The projected density operator in the lowest band is

$$PXP = \frac{1}{\sqrt{N_s}} \sum_k u_{k\alpha}^{n_1 \star} u_{k+\Delta q}^{n_2} \gamma_{n_1 k}^\dagger |0\rangle \langle 0| \gamma_{k+\Delta q}^{n_2} = \rho_{\Delta q}. \tag{C2}$$

Hence, the projected density operator for $\Delta q = 2\pi/N_x$ equals the projected position operator. There is an alternate expression for the projected position and density operators. They are translational operators in k space:

$$\begin{aligned}PXP\,|k,n\rangle = \rho_{\Delta q}\,|k,n\rangle &= u_{k-\Delta q,\alpha}^{n_1 \star} u_{k\alpha}^{n}\,|k-\Delta q, n_1\rangle \\ &\approx e^{-i \int_k^{k+\Delta q} A^{n_1,n}(k)}\,|k-\Delta q, n_1\rangle\,. \end{aligned} \tag{C3}$$

For one occupied band, the density or position operators just translate the band at different momentum, whereas for more than one occupied band, the translation is accompanied by a rotation. We now see that

$$\frac{2}{i} \frac{N_s^{3/2}}{(2\pi)^2} \mathrm{Tr}([PXP, PYP]X^{-1}Y^{-1}) = \frac{1}{N_s} \sum_{k,m} F_{xy}^{m,m}(k) = C. \tag{C4}$$

APPENDIX D: CHERN NUMBER OF A LANDAU LEVER

We outline how a simple calculation for the Chern number of LLL. The wave functions for the Landau levels in the continuum do not have two momenta k_x, k_y, and hence the momentum expression for the Chern number cannot be used. We obtain the Chern number as

$$C = -\frac{\hbar^2}{l^2} \lim_{\Delta_x, \Delta_y \to 0} \frac{1}{\Delta_x \Delta_y} \mathrm{Tr}[[PXP, PYP]X^{-1}Y^{-1}], \tag{D1}$$

where in the LLL we have the expressions

$$\begin{aligned}PXP &= \frac{1}{\sqrt{V}} P e^{i \Delta_x x} P = P e^{i \Delta_x (z+\bar{z})/2)} P, \\ PYP &= \frac{1}{\sqrt{V}} P e^{i \Delta_y y} P = P e^{\Delta_y (z-\bar{z})/2)} P. \end{aligned} \tag{D2}$$

LLL wave functions $\psi(z)$ have the property that $\Pi \psi(z) = 0$, where $\Pi = \Pi_x + i \Pi_y$, Π_x, Π_y being the canonical momenta in the presence of a magnetic field. We then have

$$P e^{za + \bar{z}b} P = P e^{i \frac{l^2}{\hbar}(\Pi a - \Pi^\dagger b)} e^{i \frac{l^2}{\hbar}(K^\dagger b - K a)} P, \tag{D3}$$

where we have used $z = (i l^2/h)(\Pi - K)$, $K = K_x + i K_y$, and the fact that Π commutes with K. We now need to disentangle the exponent containing $\Pi, \Pi^\dagger$ to obtain $e^{i \frac{l^2}{\hbar}(\Pi a - \Pi^\dagger b)} = e^{-i \frac{l^2}{\hbar} \Pi^\dagger b} e^{i \frac{l^2}{\hbar} \Pi a} e^{abl^2/h^2}$. Since $e^{i \frac{l^2}{\hbar} \Pi a} P = P$ and $P e^{-i \frac{l^2}{\hbar} \Pi^\dagger b} = P$, we have

$$P e^{za + \bar{z}b} P = e^{abl^2/h^2} P e^{i \frac{l^2}{\hbar}(K^\dagger b - K a)} P. \tag{D4}$$

This allows us the computation of the terms involved in the Chern number:

$$[PXP, PYP] = \frac{1}{V} e^{-\frac{\Delta_x^2 + \Delta_y^2}{4} \frac{l^2}{\hbar^2}} [P e^{i \frac{l^2}{\hbar} \Delta_x K_y} P, P e^{-i \frac{l^2}{\hbar} \Delta_y K_x} P]. \tag{D5}$$

Moreover, again after projection to the LLL, and after some algebra, we find

$$\begin{aligned}&\mathrm{Tr}[[PXP, PYP]X^{-1}Y^{-1}] \\ &\quad = \frac{1}{V} e^{-\frac{l^2}{\hbar^2} \frac{\Delta_x^2 + \Delta_y^2}{2}} \mathrm{Tr}[e^{-\frac{l^2}{\hbar^2} \frac{\Delta_x \Delta_y}{2}} e^{-i \frac{l^2}{\hbar} \Delta_x K_y} P e^{i \frac{l^2}{\hbar} \Delta_x K_y}] \end{aligned}$$

$$\times P e^{-i\frac{l^2}{\hbar}\Delta_y K_x} P e^{i\frac{l^2}{\hbar}\Delta_y K_x} - e^{\frac{l^2}{\hbar^2}\frac{\Delta_x\Delta_y}{2}} e^{i\frac{l^2}{\hbar}\Delta_y K_x} P e^{-i\frac{l^2}{\hbar}\Delta_y K_x} \times P e^{i\frac{l^2}{\hbar}\Delta_x K_y} P e^{-i\frac{l^2}{\hbar}\Delta_x K_y}]. \quad \text{(D6)}$$

We now observe that, if we write $P = \int d^2r\, |\psi(r)\rangle\langle\psi(r)|$ then the quantity $e^{-i\frac{l^2}{\hbar}\Delta_x K_y} P e^{i\frac{l^2}{\hbar}\Delta_x K_y}$ is again a projection operator P due to the fact that $e^{-i\frac{l^2}{\hbar}\Delta_x K_y}$ are translation operators. We find that $\mathrm{Tr}[e^{-i\frac{l^2}{\hbar}\Delta_x K_y} P e^{i\frac{l^2}{\hbar}\Delta_x K_y} P e^{-i\frac{l^2}{\hbar}\Delta_y K_x} P e^{i\frac{l^2}{\hbar}\Delta_y K_x}] = V$. We hence obtain

$$C = -\frac{\hbar^2}{l^2} \lim_{\Delta_x,\Delta_y\to 0} \frac{1}{\Delta_x\Delta_y} e^{-\frac{l^2}{\hbar^2}\frac{\Delta_x^2+\Delta_y^2}{2}} \left(e^{-\frac{l^2}{\hbar^2}\frac{\Delta_x\Delta_y}{2}} - e^{\frac{l^2}{\hbar^2}\frac{\Delta_x\Delta_y}{2}}\right) = 1. \quad \text{(D7)}$$

APPENDIX E: CENTER-OF-MASS DEGENERACY MISMATCH

The center-of-mass degeneracy in the FQH is $q = N_s/GCD(N_s,N_e)$ (with $N_S = N_x N_y$), while in the FCI it is $q_x q_y = [N_x/GCD(N_x,N_e)][N_y/GCD(N_y,N_e)]$. Their ratio is

$$\frac{q}{q_x q_y} = \frac{GCD(N_x,N_e)\cdot GCD(N_y,N_e)}{GCD(N_x N_y,N_e)}. \quad \text{(E1)}$$

We can easily prove that this is an integer by applying the decomposition of a number in primes p_i: $N_x = \prod_i p_i^{\alpha_i}$, $N_y = \prod_i p_i^{\beta_i}$, $N_e = \prod_i p_i^{\theta_i}$, where $\alpha_i,\beta_i,\theta_i$ are all integer powers. The ratio then becomes

$$\frac{q}{q_x q_y} = \prod_i p_i^{\min(\alpha_i,\theta_i)+\min(\beta_i,\theta_i)-\min(\alpha_i+\beta_i,\theta_i)}. \quad \text{(E2)}$$

We can now analyze the different cases to prove that all powers of p_i are positive in the above expression. Since our analysis is valid for *any* i, we drop the index. We have the cases (1) $\alpha \leqslant \theta$, $\beta \leqslant \theta$, $\alpha+\beta \geqslant \theta$, in which case $\min(\alpha,\theta)+\min(\beta,\theta)-\min(\alpha+\beta,\theta) = \alpha+\beta-\theta \geqslant 0$; (2) $\alpha \leqslant \theta$, $\beta \leqslant \theta$, $\alpha+\beta \leqslant \theta$, in which case $\min(\alpha,\theta)+\min(\beta,\theta)-\min(\alpha+\beta,\theta) = 0$; (3) $\alpha \geqslant \theta$, $\beta \leqslant \theta$, $\alpha+\beta \geqslant \theta$, in which case $\min(\alpha,\theta)+\min(\beta,\theta)-\min(\alpha+\beta,\theta) = \beta$; (4) $\alpha \geqslant \theta$, $\beta \leqslant \theta$, $\alpha+\beta \leqslant \theta$, in which case $\min(\alpha,\theta)+\min(\beta,\theta)-\min(\alpha+\beta,\theta) = \theta-\alpha \geqslant 0$; and (5) $\alpha \geqslant \theta$, $\beta \geqslant \theta$, $\alpha+\beta \geqslant \theta$, in which case $\min(\alpha,\theta)+\min(\beta,\theta)-\min(\alpha+\beta,\theta) = \theta$. We see that in all cases possible, $\min(\alpha,\theta)+\min(\beta,\theta)-\min(\alpha+\beta,\theta)$ is a positive integer which makes q divisible by $q_x q_y$.

[1] F. D. M. Haldane, Phys. Rev. Lett. **61**, 2015 (1988).
[2] C. L. Kane and E. J. Mele, Phys. Rev. Lett. **95**, 226801 (2005).
[3] B. A. Bernevig, T. L. Hughes, and S.-C. Zhang, Science **314**, 1757 (2006).
[4] L. Fu and C. L. Kane, Phys. Rev. B **76**, 045302 (2007).
[5] D. A. Pesin and L. Balents, Nat. Phys. **6**, 376 (2010).
[6] S. Rachel and K. Le Hur, Phys. Rev. B **82**, 075106 (2010).
[7] J. Wen, A. Rüegg, C.-C. Joseph Wang, and G. A. Fiete, Phys. Rev. B **82**, 075125 (2010).
[8] N. Regnault and B. A. Bernevig, Phys. Rev. X **1**, 021014 (2011).
[9] T. Neupert, L. Santos, C. Chamon, and C. Mudry, Phys. Rev. Lett. **106**, 236804 (2011).
[10] D. N. Sheng, Z.-C. Gu, K. Sun, and L. Sheng, Nat. Commun. **2**, 389 (2011).
[11] A. Sterdyniak, N. Regnault, and B. A. Bernevig, Phys. Rev. Lett. **106**, 100405 (2011).
[12] H. Li and F. D. M. Haldane, Phys. Rev. Lett. **101**, 010504 (2008).
[13] A. Kol and N. Read, Phys. Rev. B **48**, 8890 (1993).
[14] S. M. Girvin, A. H. MacDonald, and P. M. Platzman, Phys. Rev. B **33**, 2481 (1986).
[15] S. A. Parameswaran, R. Roy, and S. L. Sondhi, e-print arXiv:1106.4025 (to be published).
[16] N. Read and E. Rezayi, Phys. Rev. B **59**, 8084 (1999).
[17] R. B. Laughlin, Phys. Rev. Lett. **50**, 1395 (1983).
[18] G. Moore and N. Read, Nucl. Phys. B **360**, 362 (1991).
[19] F. D. M. Haldane, Phys. Rev. Lett. **55**, 2095 (1985).
[20] K. Sun, Z. Gu, H. Katsura, and S. Das Sarma, Phys. Rev. Lett. **106**, 236803 (2011).
[21] B. A. Bernevig and F. D. M. Haldane, Phys. Rev. Lett. **100**, 246802 (2008).
[22] F. D. M. Haldane, Bull. Am. Phys. Soc. **51**, 633 (2006).
[23] E. J. Bergholtz, J. Kailasvuori, E. Wikberg, T. H. Hansson, and A. Karlhede, Phys. Rev. B **74**, 081308 (2006).
[24] E. J. Bergholtz and A. Karlhede, J. Stat. Mech.: Theory Exp. (2006) L04001.
[25] E. Ardonne, E. J. Bergholtz, J. Kailasvuori, and E. Wikberg, J. Stat. Mech.: Theory Exp. (2008) P04016.
[26] A. Seidel, H. Fu, D.-H. Lee, J. M. Leinaas, and J. Moore, Phys. Rev. Lett. **95**, 266405 (2005).
[27] A. Seidel and D.-H. Lee, Phys. Rev. Lett. **97**, 056804 (2006).
[28] M. Hermanns, N. Regnault, B. A. Bernevig, and E. Ardonne, Phys. Rev. B **83**, 241302 (2011).
[29] A. Seidel and K. Yang, Phys. Rev. B **84**, 085122 (2011).
[30] B. A. Bernevig and F. D. M. Haldane, Phys. Rev. Lett. **100**, 246802 (2008).
[31] S. H. Simon, E. H. Rezayi, and N. R. Cooper, Phys. Rev. B **75**, 195306 (2007).
[32] R. Stanley, Adv. Math. **77**, 76 (1989).
[33] M. O.Goerbig, Eur. Phys. J. B **85**, 15 (2012).
[34] D. Podolsky and J. Avron (private communication).
[35] R. Thomale, A. Sterdyniak, N. Regnault, and B. A. Bernevig, Phys. Rev. Lett. **104**, 180502 (2010).
[36] A. Vaezi, e-print arXiv:1105.0406 (to be published).
[37] X.-L. Qi, Phys. Rev. Lett. **107**, 126803 (2011).
[38] E. Tang, J.-W. Mei, and X.-G. Wen, Phys. Rev. Lett. **106**, 236802 (2011).
[39] X. Hu, M. Kargarian, and G. A. Fiete, Phys. Rev. B **84**, 155116 (2011).
[40] F. Wang and Y. Ran, Phys. Rev. B **84**, 241103 (2011).
[41] D. Green, Ph.D. thesis, Yale University, New Haven, 2001; N. Read and D. Green, Phys. Rev. B **61**, 10267 (2000).
[42] E. Ardonne and N. Regnault, Phys. Rev. B **84**, 205134 (2011).
[43] B. Estienne and B. A. Bernevig, Nucl. Phys. B **857**, 185 (2012).